Multi-Wavelength All-Optical Regeneration Based on Self-Phase Modulation and Inter-Channel Walk-off Control in Fiber

CHONG, Kin Man

A Thesis Submitted in Partial Fulfillment

of the Requirements for the Degree of

Master of Philosophy

in

Information Engineering

The Chinese University of Hong Kong

September 2009

Acknowledgement

First and foremost, I would like to express my deepest gratitude to my thesis supervisor, Prof. Lian-Kuan Chen, for his continuous support and guidance in my research work. I have greatly benefited from the fruitful discussions with him and his valuable advices throughout my postgraduate studies. He has in-depth knowledge and creative thinking in optical communications, which have always given me directions and inspirations on my research ideas. His sincerity and persistence in work are also inspirational to me.

I would also like to thank Prof. Chun-Kit Chan. His guidance on my experimental skills and research paper writing are very helpful to me for the completion of this thesis.

It is my pleasure to have a chance to work with many talented fellow postgraduate students in Lightwave Communications Laboratory in the Department of Information Engineering. In particular, thanks must be given to Dr. Ning Deng, Dr. Ho Li and Mr. Jordan Tse, Dr. Guowei Lu and Dr. Jian Zhao for their fruitful discussions and experimental guidance. I would also like to express my thanks to my lab members including Mr. Yin Zhang, Mr. Zhenchang Xie, Mr. Yang Qiu, Mr Jing Xu, Mr. Kam-Hon Tse and Mr. Shuqiang Zhang.

At last, I am grateful to my family and friends for their long-term support, tolerance and encouragement. This thesis is dedicated to them.

Abstract

The continuous demands of transmission capacities for various kinds of broadband internet services have driven the rapid developments of the next generation WDM transmission systems in recent years. These broadband internet services require both a huge-bandwidth and a low-latency communication among users in long transmission distances. However, optical signals propagating through fiber links are subject to different kinds of propagation impairments, such as power loss, fiber dispersions and nonlinearities. As a result, regeneration of optical signals in transmission is important and of major concern in order to increase the propagation distance while maintaining the signal quality, especially for those ultra-long and submarine transmission systems.

Since O-E-O regeneration techniques are generally limited by the speed of the photodiodes and the electronics, they are neither suitable nor cost-effective for the high-capacity WDM systems. Considerable attentions have been drawn to the all-optical regeneration techniques that can operate multiple high-speed wavelength channels simultaneously in WDM scenarios. Although various kinds of all-optical regeneration schemes, based on either fiber nonlinearities or other optical effects in semiconductor devices, have been proposed and demonstrated in the past few years, most of them are based on the single-wavelength application and have difficulties in the extensions to support multiple wavelengths.

In this thesis, we propose and experimentally demonstrate a new all-optical fiber-based regeneration technique that can support regeneration for multiple WDM channels based on self-phase modulation (SPM) and inter-channel walk-off control.

The introduced inter-channel walk-off can successfully mitigate the severe nonlinear crosstalks among the WDM channels and make the multi-wavelength operation of the regenerator become feasible. In addition, we also investigate the scalability and the cascadability of our proposed regenerator in numerical simulations. The results show the upgrade feasibilities of the regeneration scheme for both the 10x10-Gb/s and the 4x40-Gb/s scenarios.

摘要

近年，隨着各種各樣的互聯網寬帶服務不斷湧現，人們對網絡傳輸容量的需求越來越大，這種需求促使了下一代光波分複用 (WDM) 傳輸系統的迅速發展。對於那些互聯網寬帶服務來說，它要求用戶之間能夠建立高帶寬和低延遲時間的長距離通信能力。但是，光信號在光纖網絡中傳輸會受到幾種不同的傳輸損耗，其中包括功率損耗，色散損耗和由光纖非線性效應產生的信號損耗等等。因此，爲了能夠保持光信號在傳輸中的質量並且延長信號的傳輸距離，光信號的再生 (regeneration) 技術是十分重要的並且值得人們的關注，特別是對於那些超長傳輸距離的海底光通信系統。

因爲基於光電轉換 (O-E-O) 的光信號再生技術受限制於光電二極管和其他電子器件的響應速度，所以這種再生技術並不適合用於高容載的光波分複用系統。因以，考慮到其成本效益，更多的注意力被轉移到開發可以同時支持多波長的全光信號再生技術上，而且這種可以支持多波長的全光信號再生技術將會更適合用於未來高容載的光波分複用傳輸系統。在過去的幾年裏，儘管人們已經提出並實驗證明了不少基於光纖非線性效應或是基於半導體器件中的光學效應的全光信號再生技術方案，但是這些技術方案大部分只限於單波長的應用，而且要把它們擴展到能夠同時支持多波長的應用存在着很大的困難。

在這篇論文中，我們提出並在實驗中證明了一種新的基於光纖的全光信號再生技術。這種技術是通過光纖中信號的自相位調制效應和對波分複用信號的時域錯開 (Timing walk-off) 控制從而實現多個波分信號的同時再生。我們在不同波分信號之間引入的時域錯開可以成功地消除基於自相位調制光再生技術中嚴重的信道間非線性干擾效應，這使得我們提出的光再生方案能夠實現多波分

信號的同時再生。除此之外，我們亦通過數字模擬研究了該光信號再生方案的可擴容性和可結連使用性。模擬結果顯示我們的方案可以升級並支持10x10-Gb/s 和 4x40-Gb/s 兩種光波分複用通信系統。

Table of contents

List of figures and tables

Chapter 1 Introduction

1.1. Overview of optical regeneration

Optical signals transmitted in the optical communication systems experience the propagation impairments, like power loss, fiber dispersions and nonlinearities, so regeneration of optical signals in transmission is crucial for maintaining the signal quality and increasing the propagation distance. The technology of optical regeneration at first is implemented in an optical-electrical-optical (O-E-O) way, in which the regenerators need to convert an optical signal into an electrical signal first, and then process that electrical signal and re-convert it into an optical signal for re-transmitting. Therefore, the data rates of the transmitted signals are limited by the speed of the electronic devices, thus limiting the scalability of transmission capacities [1]. In addition, O-E-O regenerators are only suitable for single-wavelength operation.

The advent of optical amplifiers has led to a breakthrough in the evolution of optical communication systems to support ultrahigh capacities in long transmission distances. The optical transmission systems, now making use of optical amplification for increasing the repeater spacing and of wavelength-division multiplexing (WDM) for increasing the bit rate, can achieve the bit rate-distance product (BL) of up to 10,000 (Tb/s)-km [1]. In order to overcome the signal quality degradation caused by the propagation impairments for those high data-rate signals, another revolution of the regeneration technology, which can regenerate the degraded signals without the limitation of the speed of electronics, is soon required. Promising developments concern in-line all-optical regeneration, which can make it possible to transmit very

high speed optical data in an ultra-long distance [2].

It should also be mentioned that electronic distortion compensation (EDC) is another emerging technology as a solution to combat those propagation impairments and extend the transmission distances. However, the robust and high-performance electronic equalization techniques require relatively complex signal processing algorithms. Since the target data rates are high (several tens of Gb/s), the highly complicated architectures of the electronic equalizers could be unfeasible to implement, due to the speed limitations of the semiconductor-based devices and high power consumptions. As a result, electronic distortion compensations demonstrated so far for high data-rate operations are mostly limited in offline processing. The real-time high-speed electronic equalizers require both efficient signal processing algorithms and technological breakthroughs in semiconductor devices [41].

In general, optical regeneration can be classified into three categories by 3R's in both the O-E-O and all-optical implementations [2]. The 3R's correspond to the three basic signal-processing functions respectively, i.e., re-amplification, re-shaping, and re-timing, as shown in Fig. 1.1 [3]. Thus the optical amplification provides "1R" regeneration. The regenerator which has both re-amplifying and re-shaping capabilities is usually referred to as a "2R" regenerator when re-timing is not present. Full 3R regeneration with re-timing capability requires clock extraction, which can be done in both electronic and all-optical way. It should be noted that optical 3R techniques are not necessarily void of any electronic functions (e.g., when using electronic clock recovery and O/E modulation), but the main feature is that these electronic functions are narrow-band (as opposed to broadband in the case of optoelectronic regeneration) [3].

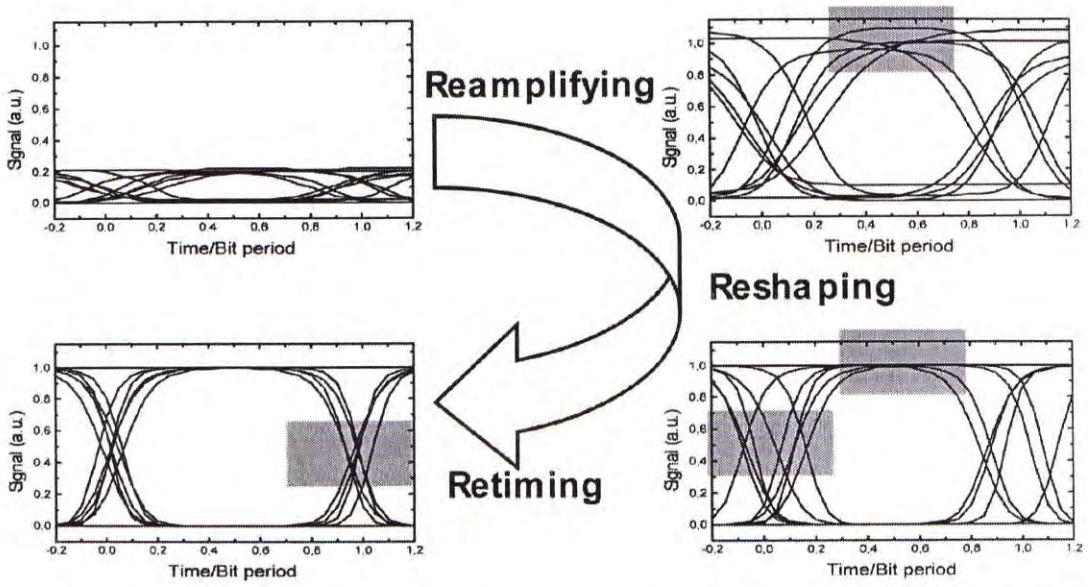

Fig. 1.1 Illustration of optical 3R regeneration for non-return-to-zero (NRZ) amplitude-modulated signals [3].

1.1.1. O-E-O regeneration

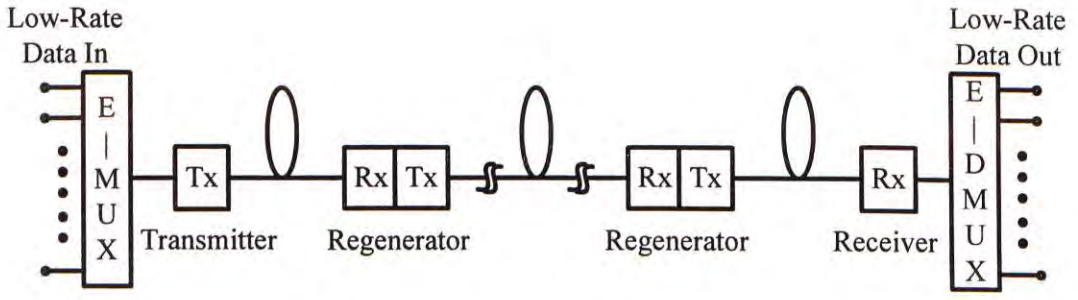

Fig. 1.2 Traditional point-to-point fiber links with periodic O-E-O regenerators. E-MUX: electrical multiplexer; E-DMUX: electrical de-multiplexer.

Fig. 1.2 shows the traditional point-to-point optical fiber transmission systems using

O-E-O regenerative repeaters. As seen in Fig. 1.2, the low-rate data of different users are first multiplexed in the electrical domain into an aggregate TDM signal, and then the multiplexed electrical signal is used to drive the transmitter laser. The O-E-O regenerators are inserted periodically in the fiber link for signal restoration. Actually an O-E-O regenerator is nothing but a receiver-transmitter pair that detects the incoming optical signal, recovers the electrical bit stream, and then coverts it back into optical form by modulating an optical source. This kind of regenerator is usually a variable-input, fixed-output converter because it does not usually care about the input signal wavelength, as long as it is in the 1310- or 1550-nm window [2].

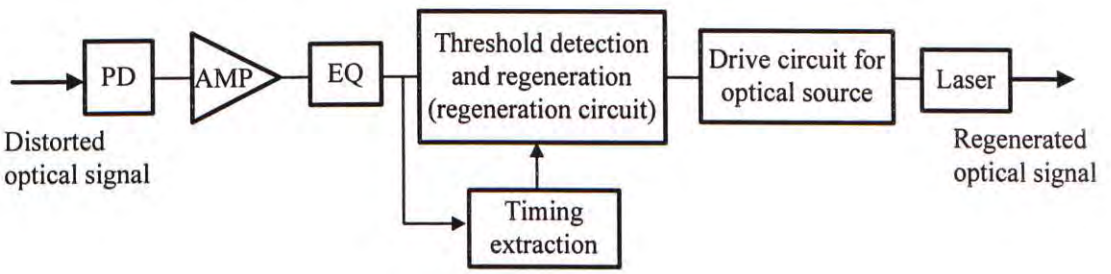

Fig. 1.3 Functional blocks of a typical O-E-O regenerative repeater. PD: photodiode; AMP: electrical amplifier; EQ: electrical equalizer.

Detailed functional parts of a typical O-E-O regenerative repeater are shown in Fig. 1.3 [4]. The distorted optical signals are detected and amplified in the receiver unit. This consists of a photodiode followed by a low noise preamplifier. The electrical signal thus acquired is given a further increase in power level in a main amplifier prior to re-shaping in order to compensate for the transfer characteristic of the optical fiber using an equalizer. Accurate timing information is then obtained from the amplified and equalized waveform using a timing extraction circuit such as a ringing circuit or a phase locked loop. This enables precise operation of the regeneration circuit within the

bit intervals of the original optical signals. The function of the regeneration circuit is to re-construct the originally transmitted pulse train, ideally without error. This can be achieved by setting a threshold above which a binary one is obtained, and below which a binary zero is recorded. The signal data are then regenerated in their original form (either a binary one or zero) before re-transmission as an optical signal driven by an electronic circuit. Since the O-E-O repeater recovers the original electrical bit stream in the regeneration, signal distortion and noises do not accumulate in fiber transmission and this is one big advantage of using the O-E-O regeneration.

However, as what we have mentioned, the disadvantage of the O-E-O repeaters is that the capacity upgrade requires high-speed electronics which are very expensive and difficult to be fabricated. Also, since the O-E-O repeater is only suitable for single-wavelength operation, it is not desirable in the implementation of modern WDM systems as it requires a lot of devices.

1.1.2. All-optical regeneration

In order to avoid a traditional O-E-O configuration, an alternative way of doing regeneration in transmission links is through all-optical method without the need of broadband electronics and converting the optical signals back and forth. Fig. 1.4 shows the point-to-point WDM transmission system using all-optical regenerators.

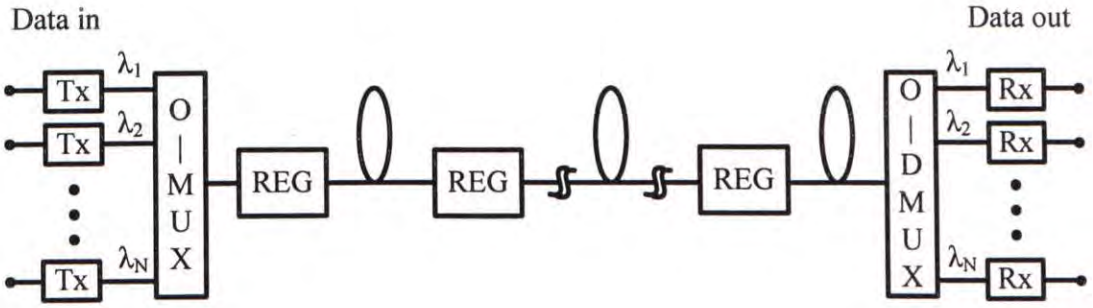

Fig. 1.4 Point-to-point WDM transmission system using all-optical regenerators. Tx: laser transmitter; Rx: optical receiver; REG: all-optical regenerator.

To be specific, all-optical regenerations can be realized by nonlinear processes and other optical effects in fiber-based devices and semiconductor-based devices [5-11]. Among them, the regeneration schemes based on fiber nonlinear effects seem to be more promising since they can support ultra-high data-rate signal regeneration (up to 120 Gb/s, 3x43-Gb/s WDM channels [18]), thanks to the ultrafast response time of fiber nonlinearities [19]. In recent years, all-optical regeneration has been investigated and demonstrated based on either fiber nonlinear processes like self-phase modulation (SPM) [5,18], cross phase modulation (XPM) [20] and four-wave mixing (FWM) [6], or some other optical effects in semiconductor devices like cross-gain modulation (XGM) [11] and cross-absorption modulation (XAM) [15]. However, many of them are focused on single-wavelength operation and only suitable for OTDM scenarios. For WDM systems, it is noted that an all-optical regenerator that can operate multiple wavelength channels simultaneously can be implemented in a brute-force way [3] , i.e., to use one all-optical regenerator for each wavelength channel. However, this not only increases system complexity but also not power-efficient and cost-effective, so it is more desirable if all wavelength channels in the WDM systems can share just a single all-optical regenerator. And this becomes the

challenge and goal for the development of the modern all-optical regeneration technologies.

1.2. Motivation of this thesis

With increasing demands of network capacities for the worldwide ever-growing broadband services, high speed all-optical communication systems have been under increasing developments in recent years. Those networking services, including real-time video and voice signals distribution, online gaming, internet services and many other multimedia services, require a huge-bandwidth and low-latency communication among users in long transmission distances. Therefore, wavelength-division multiplexing (WDM) has been more and more attractive and promising as it allows multiple wavelength channels of information to be transmitted over the same fiber link as this leads to a multiplication of the transmission capacity. Currently, the total capacity of a WDM system can ultimately exceed 30 Tb/s if the "dry" (OH peak eliminated) fibers are used [1]. Since the O-E-O regenerators are limited by the speed of the photodiodes and the electronics, considerable attention has been drawn to the all-optical regeneration techniques that can support multiple high-speed wavelength channels simultaneously in order to extend the transmission distance in the high-capacity WDM systems, especially for submarine ones.

As what we have mentioned earlier, all-optical regeneration techniques based on fibers and semiconductor devices are considered as promising solutions to meet the ever-increasing bandwidth requirement for next generation WDM transmission systems. However, many of them demonstrated can support only one wavelength channel and hence this makes the multi-wavelength all-optical regeneration still a big

challenge and far from real implementations.

The single-wavelength optical 2R regeneration exploiting the self-phase modulation (SPM) induced spectral broadening in highly nonlinear fiber (HNLF) followed by offset filtering (also known as the Mamyshev technique [5]) has attracted much attention in the past few years because of its simplicity and robustness [21-23]. However, the direct extension of this kind of regenerator for multi-wavelength applications is very challenging due to the severe nonlinear inter-channel crosstalks, i.e., cross-phase modulation (XPM) and four-wave mixing (FWM). To date, only a few schemes have been proposed to enable the multi-wavelength operation of the Mamyshev regenerator, including to utilize a suitable design of the fiber dispersion map as well as large channel spacing to induce fast walk-off time among different WDM channels [18,24,25] , or to employ the bidirectional propagation in a polarization maintaining HNLF with the polarization control [26] to mitigate the nonlinear crosstalks.

To overcome those nonlinear inter-channel impairments, we propose a new scheme in which proper timing walk-offs are introduced on different WDM channels. This can avoid the time-domain-overlapping of the wavelength channels and hence the nonlinear inter-channel crosstalks can be effectively mitigated [27]. In addition, as bidirectional fiber configuration is used in the regeneration, the number of supported channels is increased.

In summary, multi-wavelength optical regeneration based on SPM and inter-channel walk-off control is proposed and experimentally demonstrated in this thesis. The scalability and the cascadability of our proposed regenerator are further

investigated in numerical simulations.

1.3. Outline of this thesis

The remaining chapters of this thesis are organized as the following:

Chapter 2 illustrates the basic principle of all-optical regeneration and reviews some previous regeneration schemes based on SPM, FWM in fibers, and XGM, XAM in semiconductor devices.

Chapter 3 is the experimental demonstration of our proposed multi-wavelength optical 2R regenerator based on SPM and inter-channel walk-off controls that can support four 10-Gb/s RZ-OOK WDM channels. The effects of the improper filter offset and timing walk-off on the regenerator performance are also discussed.

Chapter 4 investigates both the scalability and the cascadabiltiy of our proposed multi-wavelength regenerator in numerical simulations. Simulation results of the regeneration schemes for both the 10x10-Gb/s and the 4x40-Gb/s capacity upgrade scenarios are given and discussed.

Chapter 5 is the summary of this thesis. Some possible extensions of our future research efforts such as the experimental demonstration of our regenerator to support 40-Gb/s WDM signals and the technique of multi-wavelength tunable delay are discussed.

Chapter 2 Previous schemes of all-optical regeneration

2.1. Introduction

Nonlinear and other optical effects in optical fibers and semiconductor devices offer a variety of functions in all-optical signal processing such as all-optical logic gates [28-30], high data-rate OTDM signal de-multiplexing and switching [31-33], wavelength conversion [34-36], and all-optical signal regeneration [5-10], etc.

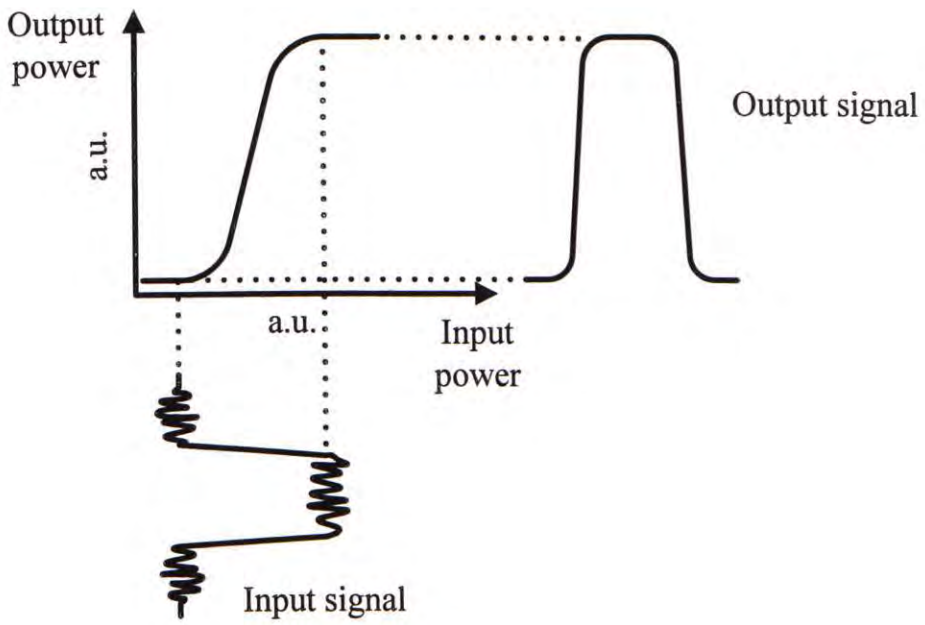

Fig. 2.1 Illustration of optical waveform re-shaping utilizing the step-like power transfer function

The working principle of all-optical regeneration techniques based on fibers or semiconductor devices is generally making use of the step-like power transfer function

obtained in those processes [3]. Fig. 2.1 is the illustration of the optical waveform re-shaping based on the step-like power transfer function. In the figure we can see that the amplitude fluctuations on both space and mark levels of the input optical pulse are eliminated by the flat response regions at the low and high power levels of the power transfer function, respectively. And it can be noted that the quality of the re-shaping behavior is actually dependent of the shape of the power transfer function. The best regeneration performance is obtained with an ideal step power transfer function. Fig. 2.2 shows the evolution of the bit-error rate (BER) versus the number of concatenated regenerators with different power transfer functions [3]. In case (a) with an ideal step function, BER is only degraded slightly even for large number of regenerators in the cascade. On the contrary, when the power transfer function is away from the ideal case, as shown in case (b) or (c), the BER degrades rapidly until the concatenation of the transfer functions reaches some steady-state pattern.

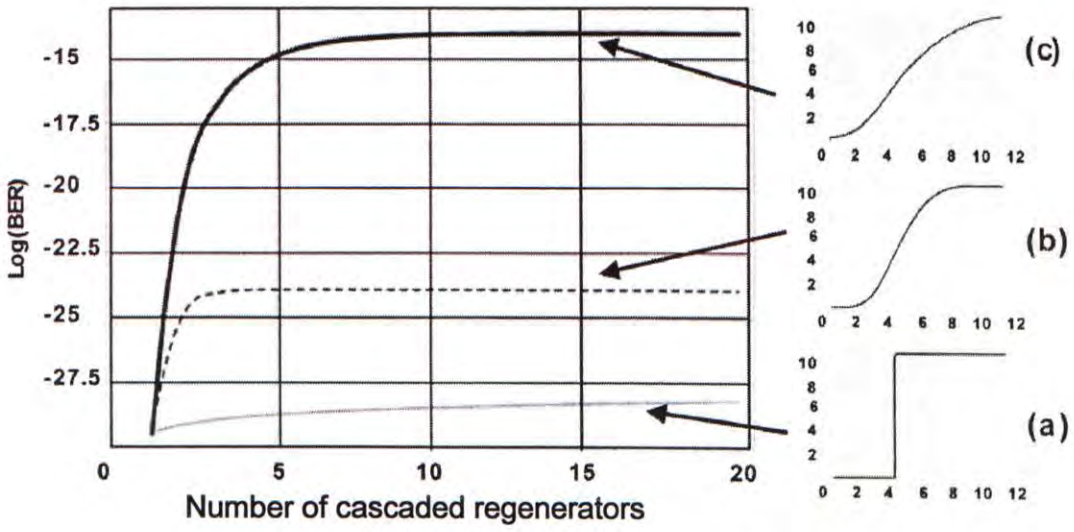

Fig. 2.2 Evolution of the BER versus the number of concatenated regenerators with different power transfer functions [3].

As mentioned above, nonlinear and optical effects in fibers or semiconductor

devices that can provide a step-like power transfer function for the input and output signals can be used to realize the all-optical regeneration function. Therefore, the major research interest of this topic mainly focuses on the following three aspects: 1) how to achieve a sufficiently good step-like power transfer function by using the nonlinear and other optical effects in fibers and semiconductor devices; 2) how to realize the full "3R" regeneration when the clock extraction can be provided; 3) how to implement the multi-wavelength supported regeneration in the WDM scenarios, instead of a single-wavelength operation.

2.2. Fiber-based all-optical regeneration

In this section, we will review some common regeneration techniques based on the nonlinear effects in fibers. Those techniques include the schemes utilizing self-phase modulation (SPM) with offset filtering [5,18,21] and the schemes employing the high-order idlers for regeneration in four-wave mixing (FWM) process [6-9].

2.2.1. SPM-based regeneration

All-optical regeneration based on SPM-induced spectral broadening followed by offset filtering (also known as the Mamyshev technique) was first demonstrated by P. V. Mamyshev in 1998 [5]. This method can suppress the noise in space levels and the amplitude fluctuations in mark levels of return-to-zero (RZ) amplitude modulated optical data streams. The principle of the technique can be described as follows. Due to the effect of SPM, the spectral bandwidth of the input RZ pulses is broadened:

$$\Delta\omega_{SPM} = \Delta\omega_0 (2\pi/\lambda) n_2 I_P L . \qquad (2.1)$$

Where $\Delta\omega_0$ is the spectral bandwidth of the input signal, I_P is the pulse intensity,

n_2 is the nonlinear refractive index, λ is the wavelength and L is the length of the nonlinear medium. After the nonlinear medium, the pulses pass through the optical filter with center frequency ω_f, which is shifted with respect to the input signal carrier frequency ω_s,

$$\omega_f = \omega_s + \Delta\omega_{shift}. \tag{2.2}$$

If the spectral broadening of the input pulse induced by SPM is small enough, i.e., when

$$\Delta\omega_{SPM}/2 < \Delta\omega_{shift}, \tag{2.3}$$

the pulse is rejected by the filter. This happens when the pulse intensity I_P is too small (noise in space levels). If the pulse intensity is high enough such that

$$\Delta\omega_{SPM}/2 \geq \Delta\omega_{shift}, \tag{2.4}$$

a portion of the SPM-broadened spectrum can pass through the filter and the spectral bandwidth of the filtered pulse is determined by the filter bandwidth $\Delta\omega_f$. Fig. 2.3 shows the schematic diagram of the regenerator.

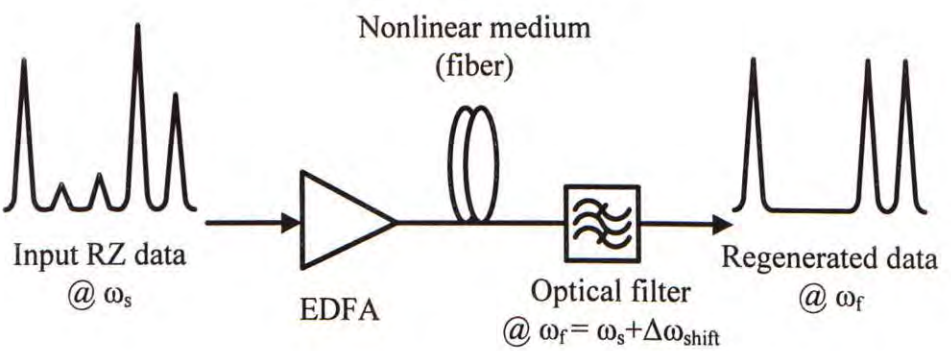

Fig. 2.3 Architecture of the regenerator based on SPM and offset filtering.

By changing the filter spectral bandwidth $\Delta\omega_f$, the output signal's pulsewidth can be

adjusted. In particular, if $\Delta\omega_f \sim \Delta\omega_s$, the output signal pulsewidth is the same as the input pulsewidth. And the intensity of the output pulse I_{out} after the spectral filtering is proportional to the spectral density I_ω of the SPM-broadened spectrum at the output of the nonlinear medium. Since $I_\omega \equiv dI/d\omega$, from (2.1) one can estimate:

$$I_\omega \sim I_P / \Delta\omega_{SPM} = \lambda/(\Delta\omega_0 2\pi n_2 L). \tag{2.5}$$

As can be seen, I_ω and the intensity of the output pulse I_{out} are independent of the input pulse intensity I_P. Therefore, the step-like power transfer function of this kind of regenerator can be established:

$$I_{out} = 0, \text{ if } I_P < I_{CR} \tag{2.6}$$

$$I_{out} = \text{constant, if } I_P > I_{CR} \tag{2.7}$$

where critical pulse intensity I_{CR} is determined from $\Delta\omega_{SPM}(I_{CR})/2 = \Delta\omega_{shift}$. Fig. 2.4 shows the power transfer functions of the single-stage and the double-stage regenerators obtained in our numerical simulations. The HNLF used in our simulations is 2 km in length and has the zero-dispersion wavelength (ZDW) of 1550 nm, the dispersion slope of 0.019 ps/nm^2/km and the nonlinear coefficient of 10.5 W^{-1} $\cdot$ km^{-1} respectively. The filter offset was optimized in the simulations. It can be observed that the double-stage regeneration yields a more step-like transfer function and thus gives a better regeneration performance. In [21], the two-stage regenerator has been successfully demonstrated using just one highly nonlinear fiber (HNLF) in bidirectional fiber configuration and 1,500-km transmission of 40-Gb/s OTDM signal with acceptable signal quality was achieved by using the cascade of the regenerators.

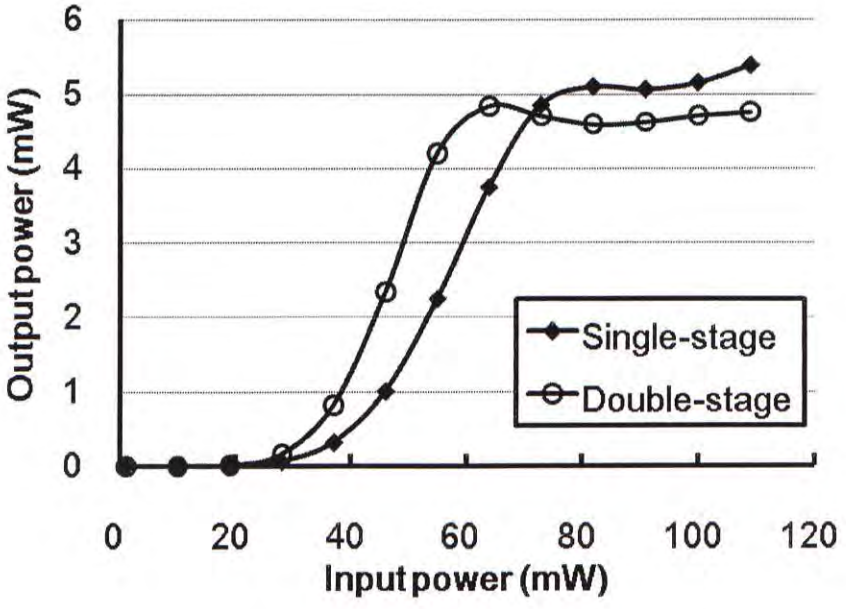

Fig. 2.4 Power transfer functions of the single-stage and the double-stage regeneration in our numerical simulations.

The advantages of this kind of regeneration scheme are mainly its simplicity and robustness. However, it should be mentioned that the SPM-based regenerator is only applicable to the RZ-OOK signals due to the power requirement in the SPM process. And this regenerator is difficult to be extended to support regeneration for multiple wavelength channels due to the severe nonlinear inter-channel crosstalks, i.e. XPM and FWM, in WDM regimes. In the next chapter we will discuss how to extend this SPM-based regenerator to operate multiple WDM channels by applying the inter-channel walk-off control.

2.2.2. FWM-based regeneration

FWM is a third-order nonlinearity in silica fibers and happens physically when three optical signals of different frequencies co-propagate inside the nonlinear medium. In FWM, the three optical frequencies will interact to produce a fourth frequency by a

relation [1],

$$\omega_4 = \omega_1 \pm \omega_2 \pm \omega_3 . \tag{2.8}$$

Several frequencies corresponding to different plus and minus sign combinations are possible in principle. In practice, by launching two signals of different frequencies ω_1 and ω_2 into a nonlinear medium, infinite number of idlers can be generated at new frequencies $\omega_1 + N(\omega_1 - \omega_2)$. These higher order idlers are generated by FWM between the generated idlers and the pump. Fig. 2.5 shows the new frequency idlers generated by FWM in nonlinear fiber.

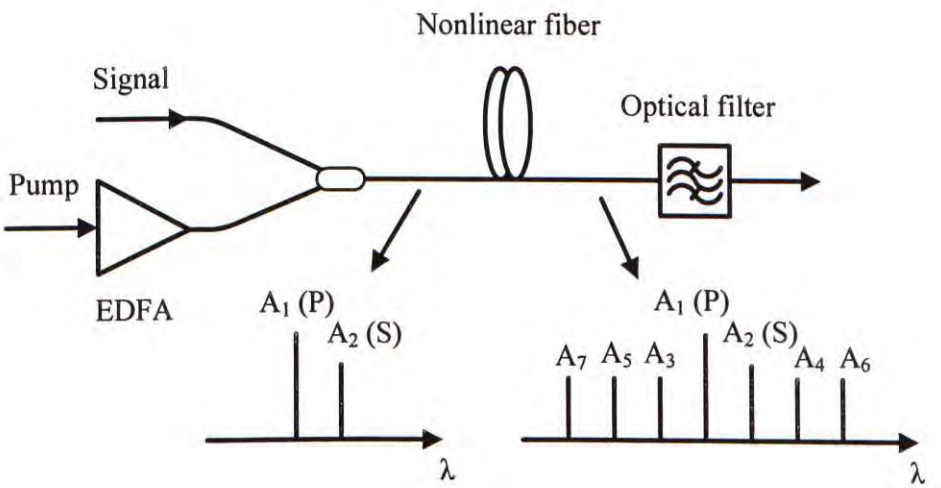

Fig. 2.5 New frequency idlers generated by FWM in nonlinear fiber.

Regeneration of the signal can be obtained by selecting the higher-order idlers, instead of the first-order idler (A_3), produced in the FWM process thanks to the step-like power transfer characteristics of the higher-order frequency components [6,7]. Physically, the regenerative properties of the higher-order idlers in FWM can be describe as follows, i.e., noise compression of the signal on space levels arises because of the characteristic dependence of the FWM-generated waves on low input power. On the other hand, when pump depletion leads to FWM gain saturation, a power plateau

can be provided for noise compression on mark levels as well. Fig. 2.6 gives our numerical simulation results of the power transfer characteristics of the 4- and 5-order idlers generated by FWM in fibers. The HNLF used in our simulations is 2 km in length and has the zero-dispersion wavelength (ZDW) of 1550 nm, the dispersion slope of 0.019 ps/nm^2/km and the nonlinear coefficient of 10.5 $W^{-1} \cdot km^{-1}$. The pump and the signal were set at the wavelength of 1550 nm and 1548.8 nm respectively in the simulations. As can been seen in the figure, the 5-order idler would offer better regeneration of the signals on both space and mark levels but at the cost of the signal power.

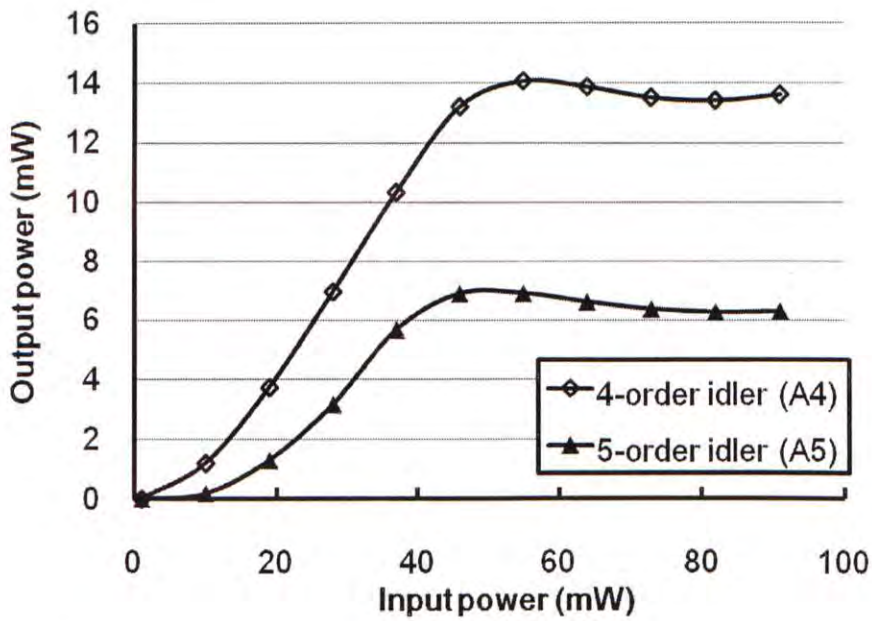

Fig. 2.6 Power transfer characteristics of the 4- and 5-order idlers in FWM in our numerical simulations

This kind of FWM-based regenerator can be applied to both RZ-OOK signals and NRZ-OOK signals and is capable to preserve their modulation formats depending on whether a continuous-wave (CW) pump is used. However, the signal wavelength is

converted after the regeneration, so it needs to be converted back if the wavelength-preserving operation is required. It is also noted that the extension of multi-wavelength operation for this kind of regenerator is not that straight-forward although the multiple-wavelength conversion is not a problem. This is because the pump depletion, which results in FWM-gain saturation, is shared by several wavelength channels simultaneously in the multi-wavelength case and thus affecting the noise suppression of the signals on mark levels.

2.3. Semiconductor-based all-optical regeneration

In addition to the fiber-based all-optical regenerators, some optical effects like XGM and XAM in semiconductor devices can also be utilized for optical signal regeneration [11-17]. The advantages of the semiconductor-based all-optical regenerators are generally compact in size, power efficient and easy for device integrations, as compared to the fiber-based ones.

2.3.1. XGM-based regeneration

Semiconductor optical amplifiers (SOAs) have been extensively studied and used for optical signal processing. Functionalities such as wavelength conversion, logic gates and optical regeneration have been demonstrated using SOAs in the past. However, operations above 40 Gb/s is always a challenge and difficult to achieve with SOA due to its slow gain recovery time. Recently, the development of the quantum-dot-SOAs (QD-SOAs) has enabled the operations of optical signal processing at higher bit rates (40 Gb/s) [13]. Various schemes of all-optical signal regeneration based on XGM in SOA have been proposed and demonstrated [11-14]. Fig. 2.7 shows the optical 2R

regeneration scheme of using two QD-SOAs in a Mach-Zehnder interferometer configuration [14].

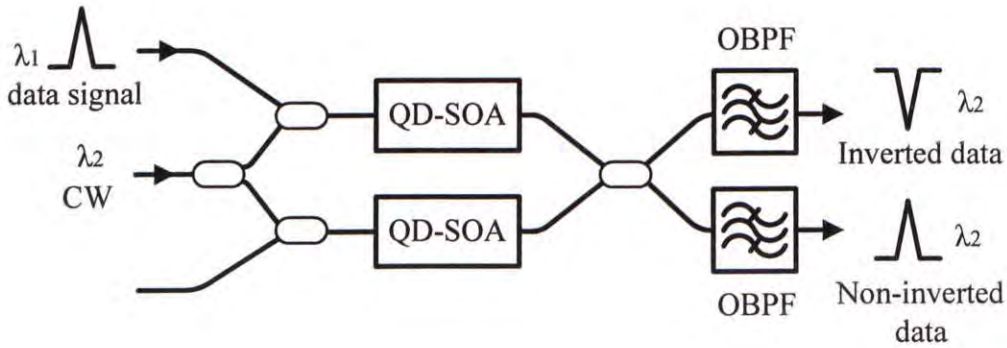

Fig. 2.7 XGM-based optical 2R regenerator in a MZI-QDSOA configuration.

As can be seen in Fig. 2.7, a continuous wave (CW) signal at wavelength λ_2 is fed into both QD-SOAs through the couplers. The data signal at λ_1 is launched only into the upper SOA and it will modulate the gain of the upper amplifier. The output coupler acts as an adder (or subtractor) in the constructive (or destructive) output port. Therefore, an inverted replica of the input signal due to XGM is obtained in the constructive port and a non-inverted one in the destructive port. The optical band-pass filters are used to select the signals at λ_2. Increasing the pump signal power drives the SOA into deeper saturation and thus the regenerative effect on mark levels is realized. However, the noise on space levels of the signals cannot be effectively reduced in the single-stage regenerator. Therefore, a second-stage regeneration, with input of the inverted regenerated signal coming from the first stage, is required for the noise suppression on space levels of the original signal. It is noted that the interferometric structure is used in the regeneration so the scheme is subject to the stability problem. In addition, the wavelength of the regenerated signal is not preserved after regeneration and the multi-wavelength application of the scheme is also challenging because the

SOA gain saturation is shared by all the channels in the multi-wavelength case and hence the noise suppression capability is limited.

2.3.2. XAM-based regeneration

Electro-absorption modulator (EAM) is becoming a more and more important device in recent years owing to its strong nonlinear absorption property and high ON-OFF ratio. Optically controlled EAMs have found a wide range of applications in wavelength conversion [37], 3R regeneration [38], and all-optical de-multiplexing [39]. The all-optical signal processing ability of EAMs is attributed to their cross-absorption-modulation (XAM) property. As a high-power optical pump pulse is injected into an EAM, its absorption decreases followed by a fast recovery process at a time scale of picoseconds. At this point, the absorption variation is transferred to a low-power optical probe pulse. Fig. 2.8 (a) and (b) depicts the schemes of the 2R and 3R regeneration using XAM in DC-biased Electro-absorption waveguide (EA-WG), respectively [17].

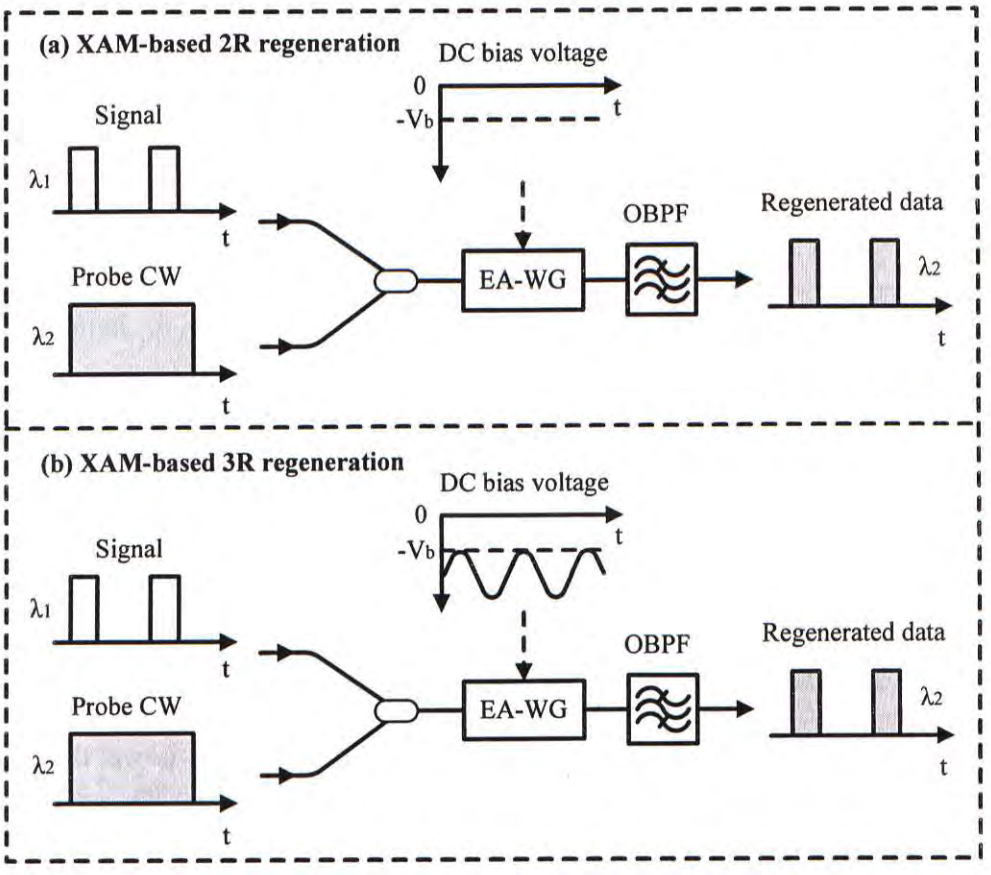

Fig. 2.8 Schemes of all-optical 2R and 3R regeneration using XAM in EA-WG.

The high-power signal light together with a probe CW is launched into the EA-WG where the cross-absorption modulation effect is induced. In the DC-biased EA-WG, the signal and the probe lights co-propagate and interact with each other. This gives rise to the modulation of the probe light by a loss variation of the EA-WG due to the cross-absorption saturation effect. During the mark periods of the launched signal, the absorption of the EA-WG is saturated because the signal has larger power at that moment. Under this condition, the probe light can pass through an EA-WG with a smaller loss. On the other hand, during the space periods of the launched signal, the absorption is tuned to an un-saturated state because the signal has smaller power. In this case, the probe light sustains a larger loss. As a result, 2R regeneration is obtained, as shown in Fig. 2.8 (a). When the timing (clock) extraction of the control signal is available, the extracted synchronized clock signal can be used to couple with the DC

bias and to drive the EA-WG. This can result in a gating effect on the amplitude-regenerated probe pulses and the timing jitter reduction of the original signal is thus realized. Therefore, all-optical 3R regeneration of the signal is achieved, as shown in Fig 2.8 (b). It is also noted that this scheme is not wavelength preserving and its extension of multi-wavelength operation is limited by the gain saturation shared by multiple wavelength channels.

2.4. Multi-wavelength regeneration

Various kinds of optical regeneration schemes based on fiber nonlinearities or other optical effects in semiconductor devices have been reviewed and discussed in the earlier parts. The reason why those schemes mainly focus on single-wavelength operation is due to the existences of their own difficulties in the extension to support multi-wavelength operation.

In particular, for the SPM-based regenerators, the main difficulty in their multi-wavelength extensions is attributed to the unwanted nonlinear inter-channel impairments in fibers caused by FWM and XPM, which are severe enough to totally degrade the incoming signals if no mitigation of those crosstalks is employed. To date, only limited number of SPM-based schemes has been proposed to support regeneration for multiple wavelength channels. Those schemes either utilized suitably designed fiber dispersion map to induce fast walk-off time on the pulses of different WDM channels or used the polarization- and direction-multiplexing in the HNLF such that those nonlinear impairments can be mitigated to enable the multi-wavelength regeneration. Regeneration of up to three 43-Gb/s WDM channels was demonstrated in [18]. On the other hand, in the FWM-, XGM- and XAM-based regeneration

schemes the amplitude-equalizing effect of the signal is mainly coming from the gain saturation effect which is shared by all channels in WDM regimes, so those schemes are not good candidates for the multi-wavelength regeneration. Two-wavelength regeneration was reported in the QD-SOA based on XGM in numerical simulations [12].

2.5. Summary

In this chapter, several previously proposed schemes for all-optical 2R and 3R regeneration are reviewed. These schemes can be mainly divided into two categories, i.e., fiber-based regeneration and semiconductor-based regeneration depending on whether fiber nonlinearities or optical effects in semiconductor devices are contributed to the signal regeneration.

For the schemes based on fiber nonlinearities, the cost is relatively low and the system architecture is generally less complex. Moreover, the fiber-based regenerators usually support high bit-rate operations thanks to the ultra-fast fiber nonlinearities. Nevertheless, the price to pay for this kind of regenerators is that: 1) high power amplification is usually needed to generate the sufficient strength of fiber nonlinear effects for the signal regeneration; 2) not suitable for device integration due to the bulky size of fibers. Therefore, power efficiency, performance stability and size are always major concerns for the fiber-based regenerators in the real implementations.

On the other hand, those semiconductor-based optical regenerators usually offer better power efficiency and potential for device integration because of their compact sizes. However, in addition to high costs, fabrications of those semiconductor devices

are difficult and require technological breakthroughs especially when the devices are required to support operations of higher and higher speed.

No matter for fiber-based regenerators, or semiconductor-based regenerators, the multi-wavelength regeneration capability is always a challenge and difficult to achieve. However, this technique is of great importance, especially in the next generation WDM transmission systems. More and more efforts are going to be put into the development of the multi-wavelength all-optical regenerators.

In the next chapter, we propose a novel scheme for multi-wavelength all-optical 2R regeneration based on SPM in bidirectional fiber configuration. In our proposed scheme, the severe inter-channel nonlinear interactions are effectively mitigated by the inter-channel walk-off control and optical 2R regeneration is successfully demonstrated for four 10-Gb/s WDM channels spaced by 300 GHz. Our numerical simulation results will be presented in chapter 5 to further show the scalability and the feasibility of the concatenated regenerators to support both the10x10-Gb/s and 4x40-Gb/s WDM systems.

Chapter 3 Multi-wavelength optical 2R regeneration utilizing self-phase modulation and inter-channel walk-off control in fiber

3.1. Introduction

As mentioned earlier, an all-optical regenerator that supports regeneration for multiple wavelength channels can be implemented in a brute-force way, i.e., to use one single regenerator for one individual WDM channel (parallel implementation). However this implementation not only increases the system complexity, but also is not cost-effective and power efficient. So what we desire is to use a single regenerator to provide regeneration on all the wavelength channels.

The single-wavelength fiber-based optical 2R regeneration based on the self-phase modulation (SPM) induced spectral broadening in highly nonlinear fiber (HNLF) followed by offset filtering (also known as the Mamyshev technique [5]) has attracted much attention in the past few years because of its simplicity and robustness [18,21,22]. However, the direct extension of this kind of regenerator for multi-wavelength applications is always a challenge due to the severe nonlinear

inter-channel crosstalks, i.e., cross-phase modulation (XPM) and four-wave mixing (FWM). To date, only a few schemes have been proposed to mitigate those nonlinear interactions among different WDM channels such that the multi-wavelength operation of the Mamyshev regenerator can be realized. Those approaches can be mainly divided into two categories. The first type relies on a suitable design of the fiber dispersion map which can induce fast walk-off time between different WDM channels, by using large channel spacing (e.g. 600 GHz). This fast walk-off time induced on the WDM channels can average out the phase shifts due to the XPM caused by the other channels, thus weakening the nonlinear inter-channel crosstalks in the regeneration [18,24,25]. The second type makes use of the polarization multiplexing in a polarization maintaining bidirectional HNLF configuration with the polarization control [26]. The polarization multiplexing separates the WDM channels in polarization and reduce their nonlinear crosstalks.

In this chapter, we propose a novel scheme in which timing walk-off on different WDM channels is controlled to avoid the overlapping of the channels in time domain such that effective mitigation of the nonlinear inter-channel impairments can be obtained, and the number of supported channels in the regeneration is increased by applying a bidirectional fiber configuration. In our scheme, optical 2R regeneration is successfully demonstrated for four 10-Gb/s RZ-OOK WDM channels spaced by 300 GHz. It is worth noted that by applying the polarization multiplexing, the number of supported channels in the scheme can be doubled and 3R regeneration can be further achieved if the synchronous modulation is added [40]. Our numerical simulation results will be given in the next chapter, showing the scalability and the effectiveness of the proposed regenerator to support both the 10x10-Gb/s and the 4x40-Gb/s WDM systems.

3.2. System architecture of the regenerator

Fig 3.1 shows the system architecture of our proposed multi-wavelength 2R regenerator based on SPM and inter-channel walk-off control.

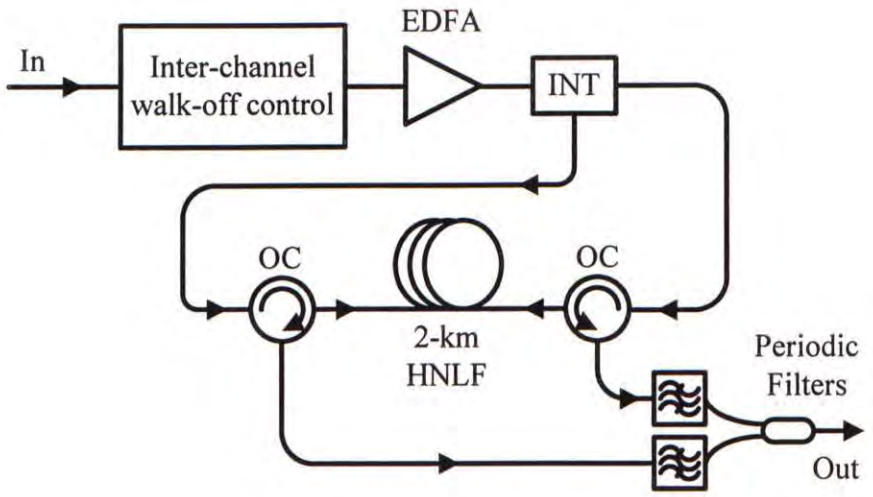

Fig. 3.1 Proposed system architecture of the multi-wavelength 2R regenerator based on SPM and inter-channel walk-off control. INT: interleaver.

The input signals to the regenerator are multiple degraded WDM signals. In order to mitigate the nonlinear inter-channel crosstalks, i.e., XPM and FWM, we introduce the timing walk-off control on different WDM channels. This control mechanism is employed to guarantee that the pulses on different wavelength channels do not have overlapping in time domain when they propagate through and induce SPM in the highly nonlinear fiber. As a result, the nonlinear crosstalks generated by XPM and FWM can be mitigated. After proper inter-channel walk-off control and amplification of the signals by EDFA, the WDM channels are interleaved into two groups and launched into the 2-km highly nonlinear fiber from the two ends for SPM-induced

spectral broadening. Here the use of the bidirectional HNLF configuration can increase the number of supported channels in the regeneration. At last, offset filtering is applied to the spectrally broadened signals from both sides of the fiber. It is noted that sufficient channel spacing between different WDM channels should be assigned to prevent the possible spectral overlapping (linear crosstalk) due to the SPM-induced spectral broadening of the WDM signals. Actually, the use of bidirectional fiber configuration also helps improve the spectral efficiency but Rayleigh backscattering effect is thus caused and needs to be investigated. In terms of the scalability of our proposed 2R regenerator, utilizing polarization multiplexing of the signals is one straight-forward approach to increase the number of supported channels in the proposed scheme, on condition that the polarization-maintaining HNLF and polarization controls are used. In addition, the increase of supported channel number can also be realized by time-interleaving more WDM channels within one signal's bit period using the inter-channel walk-off control. This method requires narrow signal pulses to prevent their timing overlapping and maintain good mitigation of the nonlinear inter-channel interactions among the WDM channels. Our numerical simulation results given in the next chapter show that our proposed regenerator can be scaled up to support the 10x10-Gb/s and the 4x40-Gb/s WDM upgrade scenarios using this inter-channel walk-off control. Actually the scalability of supported channel number of the regenerator in real implementations is limited by the EDFA bandwidth and gain.

3.3. Experimental setup

To investigate and verify the regenerative performance of our proposed multi-wavelength regeneration scheme, we have experimentally demonstrated the 2R

all-optical regeneration for four wavelength channels based on the setup shown in Fig. 3.2.

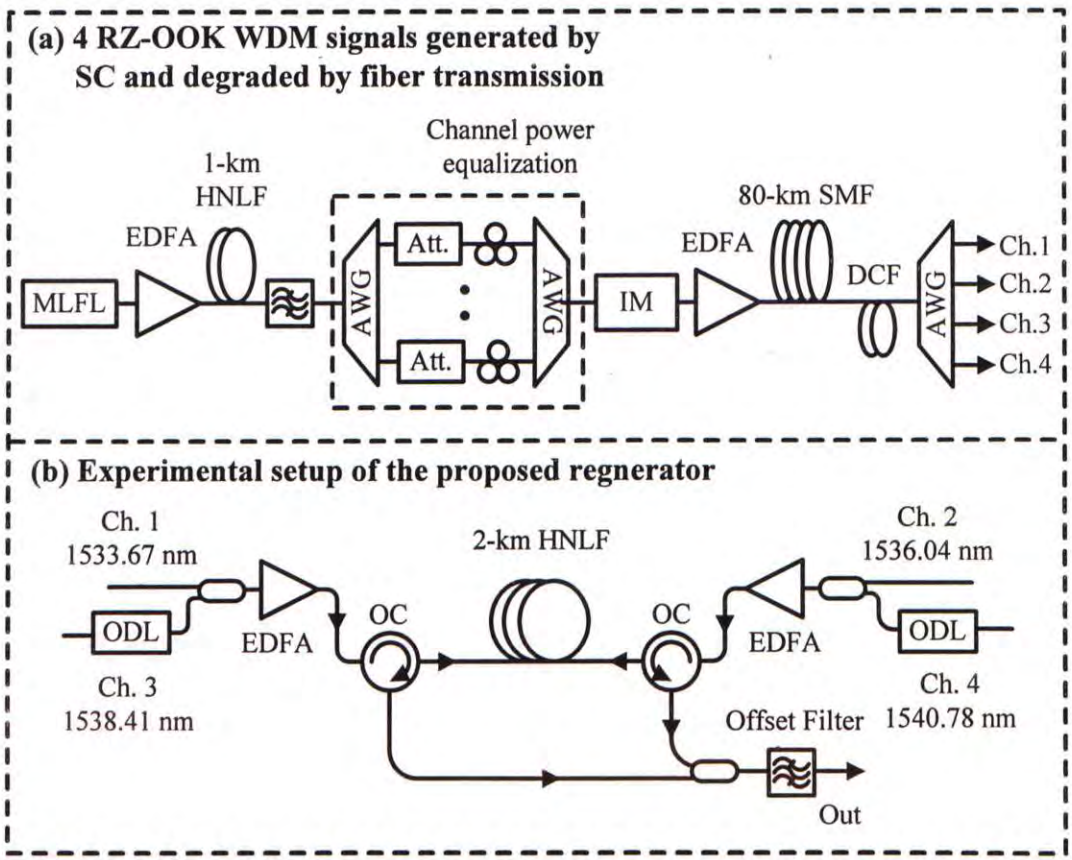

Fig. 3.2 Experimental setup. MLFL: mode-locked fiber laser; IM: intensity modulator; Att.: attenuator; ODL: optical delay line. AWG: arrayed waveguide grating.

Since narrow signal pulses with high peak power are required in the scheme to generate sufficient SPM-induced spectral broadening for signal regeneration, the four RZ-OOK WDM signals at 10 Gb/s in our experiment were generated by super-continuum followed by spectrum slicing. A mode-locked fiber laser (MLFL) at 1536 nm, with repetition rate and full-width at half-maximum (FWHM) of 10 GHz and 3.3 ps, followed by a high-power erbium-doped fiber amplifier (EDFA) was used to generate the super-continuum effect in a piece of 1-km dispersion flattened highly

nonlinear fiber (DF-HNLF), of which the zero-dispersion wavelength, the dispersion slope at 1550 nm and the nonlinear coefficient are 1550 nm, 0.01 ps/nm^2/km and 11.2 W^{-1}·km^{-1}, respectively. The average input power launched into the DF-HNLF for the super-continuum effect is 15 dBm. Fig. 3.3 (a) and (b) show the generated super-continuum spectrum of the MLFL after the 1-km DF-HNLF with and without a following 12-nm bandwidth optical band-pass filter, respectively. The optical band-pass filter was used to suppress the side modes in the subsequent spectral slicing process using the arrayed-waveguide grating (AWG).

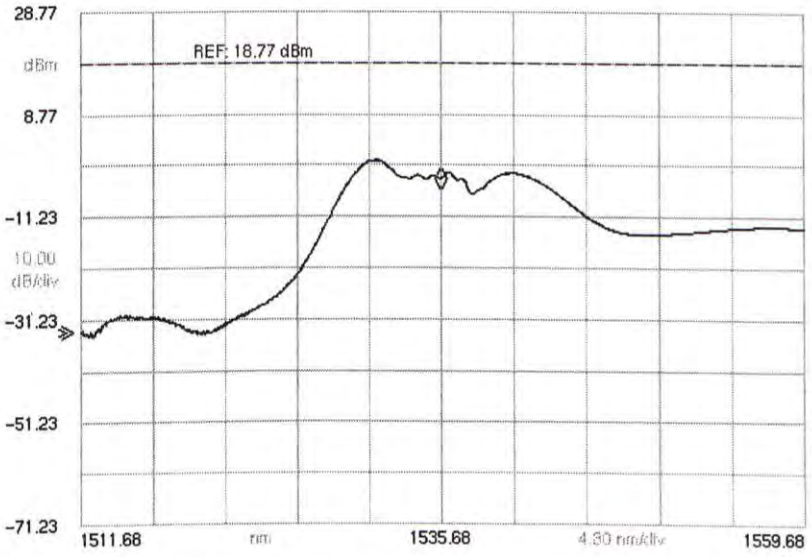

(a) without optical band-pass filter after SC

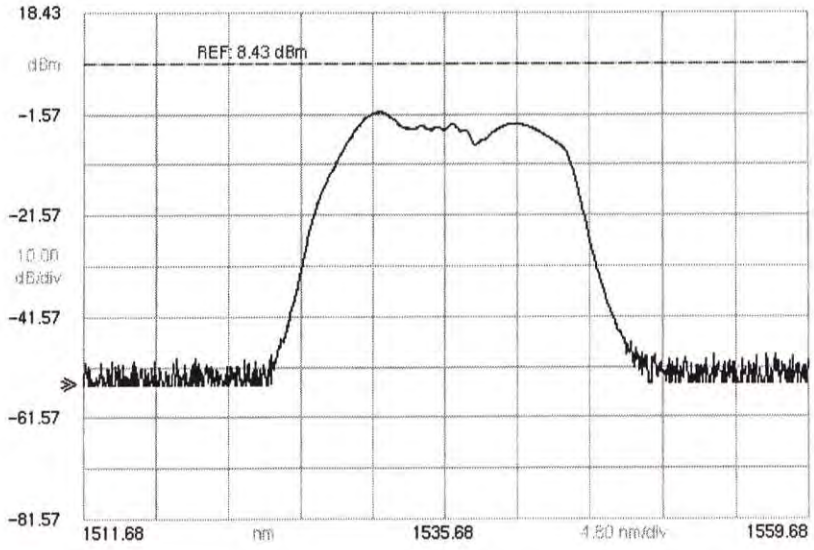

(b) with a 12-nm optical band-pass filter after SC

Fig. 3.3 Generated super-continuum spectrum of the MLFL, (a) with and (b) without a following optical band-pass filter.

The spectral slicing of the generated super-continuum spectrum was performed by a 16-port-to-16-port AWG with 100-GHz channel spacing and 0.35-nm bandwidth for individual channel. The four useful WDM signals sliced out are at the wavelength from 1533.67 nm to 1540.78 nm, spaced by 300 GHz and with FWHM of 14 ps. Channel powers were equalized to minimize the possible performance variation of the 4 channels in the later regeneration process. After the data modulation by an intensity modulator and power amplification by an EDFA, the four channels were launched into a spool of 80-km single mode fiber (SMF) followed by two dispersion compensating modules, of which the dispersions are -680 ps/nm and -666 ps/nm at 1545 nm respectively, for propagation impairments in the fiber transmission. Then the degraded WDM signals were input to the regenerator shown in Fig. 3.2 (b). The inter-channel walk-off control in this experiment was realized by using the optical tunable delay lines. It is noted that this walk-off control can also be realized by using a single piece

of SMF with suitably designed length in the actual implementation for bit-synchronous WDM signals with equal channel spacing. Since we employed the bidirectional fiber configuration, two of the four WDM signals spaced by 600 GHz were operated in each propagation direction of the HNLF and the timing walk-off between the two channels in the same propagation direction was controlled to be the optimal 50 ps for the 10-Gb/s signals.

After the signals were amplified to have the average power of around 19.8 dBm at each fiber input, they are launched into a piece of 2-km HNLF, of which the zero dispersion wavelength, the dispersion slope and the nonlinear coefficient are 1550 nm, 0.019 ps/nm^2/km and 10.5 $W^{-1} \cdot km^{-1}$ respectively, from the two sides for spectral broadening. Finally, a 0.3-nm bandwidth optical band-pass filter was used for offset filtering on the signals with 1.06-nm offset. It is worth noted that the scheme can be further upgraded to support 8 channels if polarization multiplexing is applied. Since wavelengths of the regenerated signal are shifted, even number of regenerators can be used if the wavelength-preserving inline regeneration is needed.

3.4. Results and discussions

Fig. 3.4 shows the eye diagrams of the 4 WDM channels before and after the regeneration, respectively. Those amplitude fluctuations on the signals' space levels are suppressed by the offset filtering as their power are not high enough to generate sufficient spectral broadening and hence are rejected by the filter, while the fluctuations on the mark levels is reduced since the pulses with larger power will experience larger loss and a self-regulating effect on signals' mark levels is thus obtained.

Before regeneration

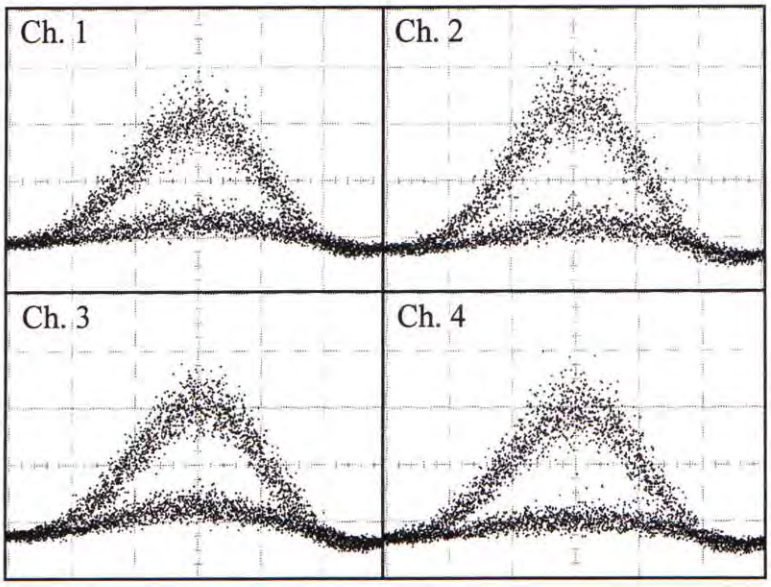

20 ps/div

After regeneration

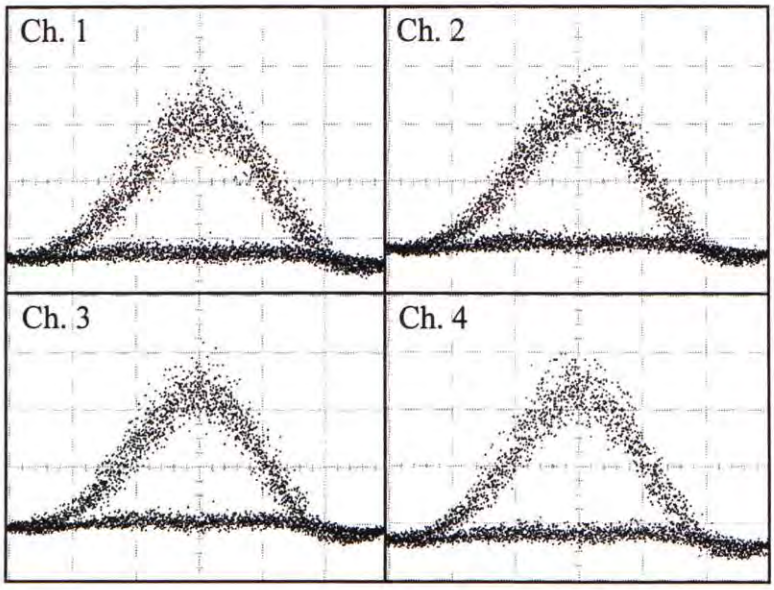

20 ps/div

Fig. 3.4 Eye diagrams of the four WDM channels before and after the regeneration.

We can see in Fig 3.4 that clear eye openings are obtained for all the channels after regeneration as the nonlinear inter-channel crosstalks are significantly mitigated, thanks to the proper inter-channel timing walk-off introduced inside the regenerator. By comparison, the signal's eye can be totally close after regeneration, as will be shown later, without the proper inter-channel walk-off due to severe nonlinear interactions among channels. Effective extinction ratio improvements on the regenerated signals with proper walk-off control can be obtained due to the successful reduction of those amplitude noises on both the mark and the space levels. BER measurement was carried out to confirm the regenerative performance of our proposed regenerator. The results are shown in Fig. 3.5. More than 4-dB improvements of the receiver sensitivity at BER of 10^{-9} were obtained for the regenerated channels. And we did not observe significant variation of the regeneration performance among different channels. In addition, no remarkable Rayleigh backscattering induced power penalty was noticed in the bidirectional fiber configuration used for the regeneration.

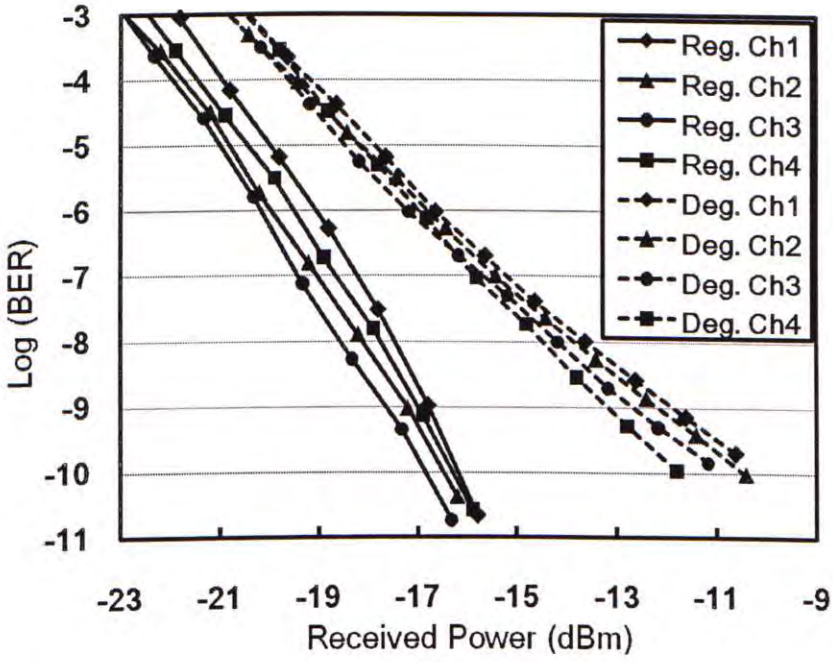

Fig. 3.5 BER measurements of the four channels before (dashed lines) and after (solid

lines) the regeneration.

3.4.1. Effects of the improper inter-channel walk-off

The performance tolerance of our proposed regenerator to the improper timing walk-offs of channels is also evaluated in our experiment. Fig. 3.6 gives the receive sensitivity of channel 1 (at 1533.67 nm) at BER of 10^{-9} versus different timing walk-off values of channel 3 (at 1538.41 nm) in the same propagation direction in regeneration.

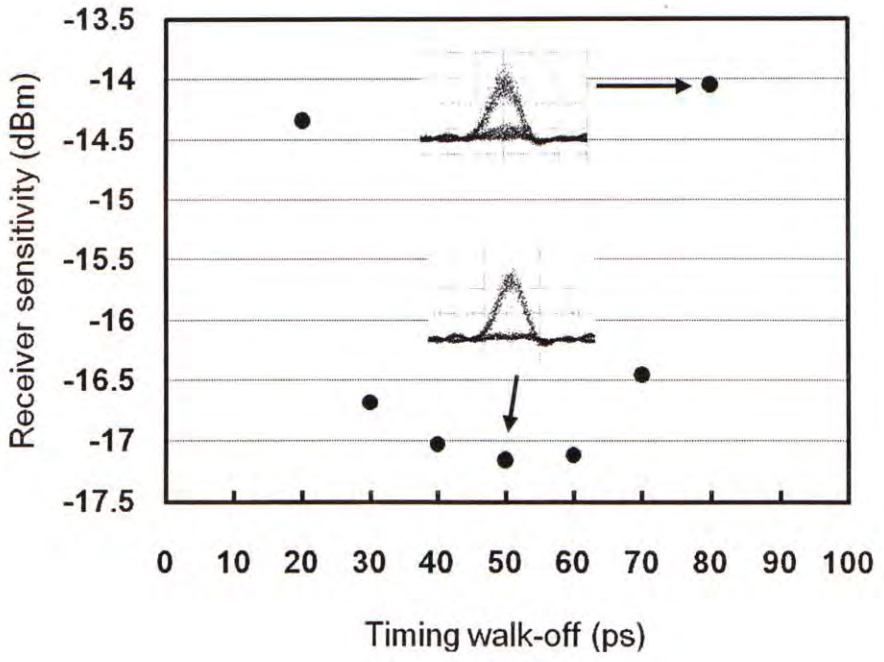

Fig. 3.6 Receiver sensivity of channel 1 at BER of 10^{-9} versus different timing walk-off values of channel 3 in the same propagtion direction in regeneration.

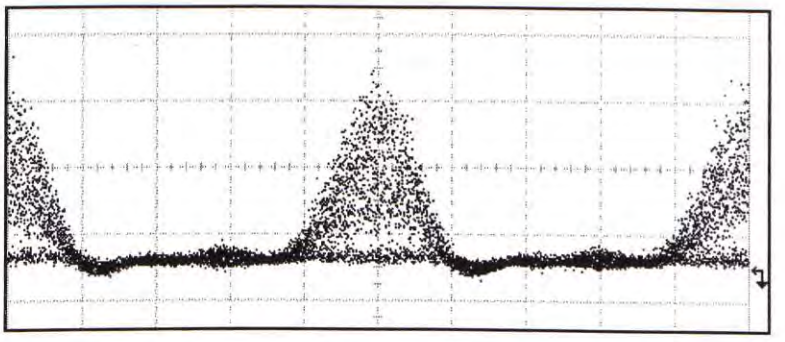

20 ps/div

Fig. 3.7 Eye diagram of one regenerated WDM channel without proper inter-channel timing walk-off.

As what we may expect, timing walk-off of around 50 ps gives the best regeneration quality of the signals due to the successful mitigation of the nonlinear inter-channel crosstalks because of the sufficient separation of the pulses on different channels in time domain. However, when the timing walk-off is further away from the optimal value, the timing overlapping of the pulses on different wavelength channels will gradually increase. This results in a dramatic increase of the nonlinear crosstalks and the signals' eyes after regeneration can become totally close, as shown in Fig. 3.7, when the pulses on different channels coincide in time domain (walk-off = 0 ps). In Fig. 3.6, we notice the eye closesure and about 3-dB power penalty of the signal when the timing walk-off is 30 ps away from the optimal value, due to the increase of nonlinear inter-channel crosstalks. It should be mentioned that proper timing walk-offs on the WDM channels are critical to the regeneration performance of our proposed scheme.

3.4.2. Effects of the improper filter offset

The frequency offset of the filter that used for offset filtering in the SPM-based regeneration is also critical to the regenerator performance. It is because when the

frequency offset of the filter is too small (the filter center is close to the signal carrier), those amplitude fluctuations on space levels of the signal may have enough power to generate sufficient SPM-induced spectral broadening and pass through the filter. This leads to an insufficient rejection of the amplitude noises on signal's space levels. Fig. 3.8 shows the eye evolution of one regenerated channel as we increase the filter offset by 0.25 nm step by step. We can see that better and better suppression of the "zero" level fluctuations can be obtained. However, it should also be mentioned that the filter offset should not be too large as the signal power will suffer after large-offset filtering. In addition, some "one" pulses with lower power levels may be rejected by the filter with large offset and thus errors are caused on the signal. Fig. 3.9 gives the receiver sensitivity of one WDM channel at BER of 10^{-9} versus different filter offsets in our experiment. The increase of receiver sensitivity when the filter offset is larger than the optimal value (1 nm) is mainly due to the increased amount of ASE noise from the EDFA used before BER measurement for pre-amplification when the signal power is small after offset-filtering. The optimal filter offset depends on the signals' peak power after EDFA as the amplified signals with different power levels can induce different strengths of SPM in the HNLF and hence have different spectral broadening. In particular, larger filter offset should be chosen for signals with larger spectral broadening, while simultaneously maintaining certain acceptable signal power in the regeneration because larger filter offset can provide sufficient noise suppression on space levels. Fig. 3.10 shows the optimal filter offset versus the signal power launched into the HNLF in our numerical simulations. In the simulations, we used the 10-Gb/s RZ-OOK signal with FWHM of 13ps at 1545.8 nm. The HNLF is 2-km long and has the zero-dispersion wavelength (ZDW) of 1550 nm, the dispersion slope of 0.019 $ps/nm^2/km$ and the nonlinear coefficient of 10.5 $W^{-1} \cdot km^{-1}$ respectively. At low signal power, the optimal filter offset remains roughly constant as no apparent regeneration

property can be obtained. Besides, it should be noted that the output signal's pulsewidth can be kept the same as the input signal's pulsewidth if an offset filter with the same spectral bandwidth as the input signal's spectrum is used.

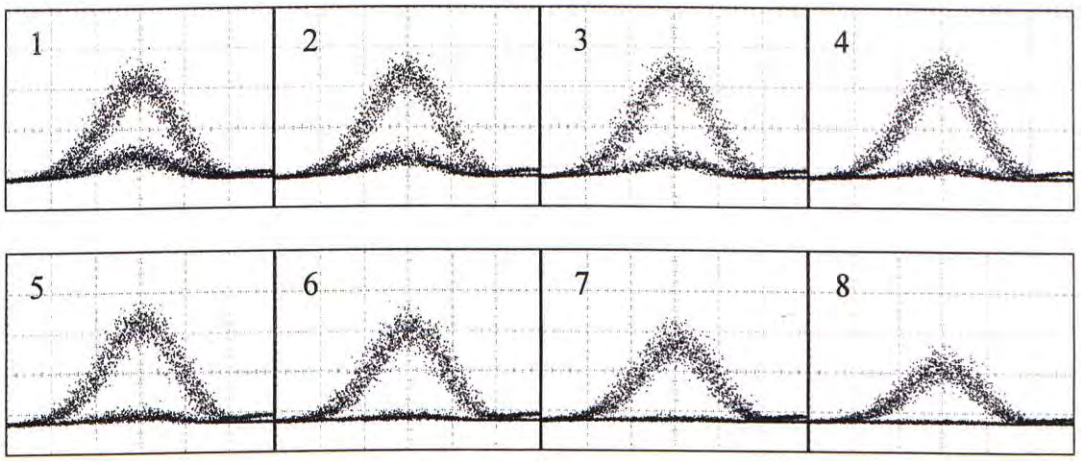

Fig. 3.8 Eye diagrams of one regenerated signal with the increase of filter offset by 0.25 nm from 1 (no offset) to 8.

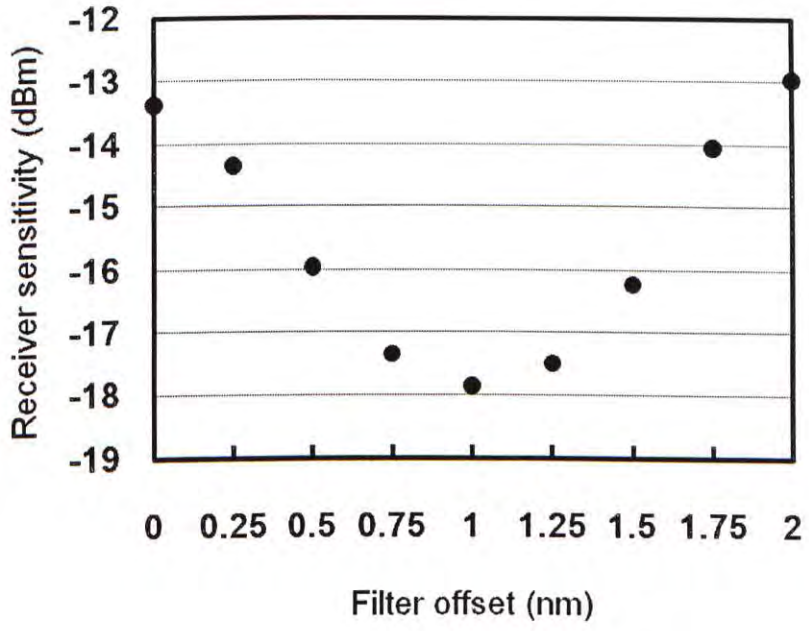

Fig 3.9 Receiver sensivity of one WDM channel at BER of 10^{-9} versus different filter offsets in the experiment.

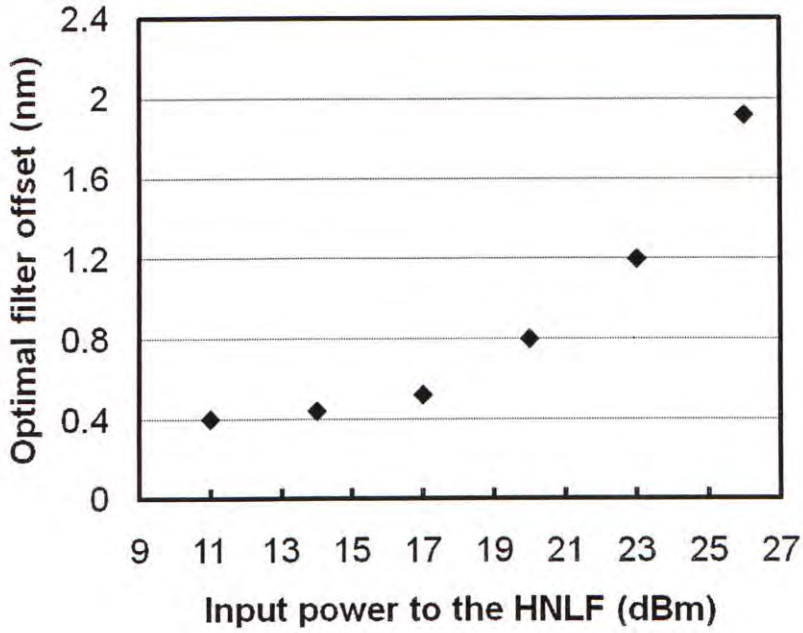

Fig 3.10 Optimal filter offset versus signal power launched into the HNLF in numerical simulations.

3.5. Summary

In this chapter, we have experimentally demonstrated optical 2R regeneration for four 10-Gb/s RZ-OOK WDM channels with 300-GHz channel spacing utilizing our proposed multi-wavelength regeneration scheme based on self-phase modulation and inter-channel walk-off control in a bidirectional fiber configuration. In the experiment, the nonlinear inter-channel crosstalks in our SPM-based regenerator are effectively mitigated because of the proper timing walk-off introduced on the WDM channels. BER measurement shows more than 4-dB improvements of receiver sensitivity at BER of 10^{-9} for the regenerated signals. In addition, the effects of improper timing walk-off and filter offset on the performance of the regenerator are also investigated. The results show that both the proper inter-channel timing walk-off and filter offset are critical to the quality of the regenerated signals.

Chapter 4 Investigation of the scalability and cascadability of our proposed multi-wavelength regeneration scheme

4.1. Introduction

Capacity upgrade of the WDM transmission systems can be achieved by either adding more wavelength channels, or increasing the bit rate of the WDM channels. As a result, an all-optical regenerator that can be scaled up to support these two kinds of capacity upgrades will be more desirable and promising. In addition, feasibility of the concatenation of the regenerators is another very important consideration because inline multi-stage regeneration is commonly needed especially in the ultra-long haul transmission systems such as the submarine ones.

In this chapter, we investigate the scalability and the cascadability of our proposed regeneration scheme with numerical simulations. In particular, for the capacity upgrade of using more wavelength channels, the regeneration can be achieved by time-interleaving more channels within one signal's bit period. On the other hand, if the capacity upgrade is done by increasing the bit rate of the WDM channels, signals with larger channel spacing are needed in the regeneration to prevent the possible spectral overlapping due to SPM. It is noted that both narrow signal pulses

and accurate inter-channel walk-off control are necessary for the regeneration in these two types of capacity upgrade. In our numerical simulations, all-optical 3R regeneration has been successfully demonstrated for both 10x10-Gb/s and 4x40-Gb/s bit-synchronous WDM channels based on the proposed regeneration scheme in addition with the synchronous modulation technique. Moreover, the use of cascaded regenerators has been proved to give a significant increase in the transmission distance with certain acceptable signal quality compared to the case without regenerators.

4.2. Simulation models and results

4.2.1. 10x10-Gb/s scenario

Fig. 4.1 shows the architecture of our proposed optical 3R regenerator in numerical simulations for the 10x10-Gb/s WDM upgrade scenarios [27].

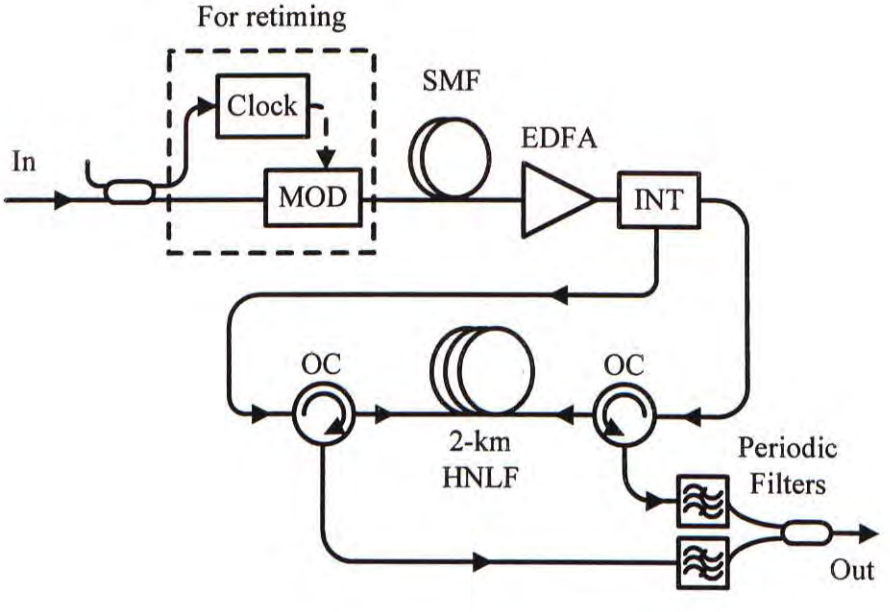

Fig. 4.1 Architecture of the proposed optical 3R regenerator for ten bit-synchronous

10-Gb/s WDM channels in numerical simulations. MOD: intensity modulator.

It is noted that only a single modulator is used to provide the synchronous modulation on all the WDM channels for re-timing purpose inside the regenerator. Bit-synchronous WDM channels are thus required and assumed in the scheme, which is applicable in the point-to-point transmission systems with proper dispersion management on condition that a single pulse carver is used for all WDM channels at the transmitter side. However, in the cases where channel add-drops are required, the bit-synchronicity of the WDM channels needs a more powerful re-synchronization scheme for the WDM signals.

In the simulation, ten RZ-OOK WDM channels at 10 Gb/s with duty cycle of 33% are launched into the regenerator. They are at the wavelength from 1534.6 nm to 1549 nm with 1.6-nm spacing (200 GHz at 1550 nm) and assumed to be aligned in bit slot at the regenerator input. A synchronous intensity modulator, which is driven by the electrical clock pulses extracted from the incoming signals, is used to apply pulse carving simultaneously on all the WDM signals such that both the pulsewidth and the timing jitter of the incoming signals can be reduced. In order to achieve a 10-channel operation, we need to operate five of them in each propagation direction in the HNLF. Therefore we split the channels into odd- and even-channel groups and launched them separately into the two ends of the HNLF, such that the channels are spaced by 3.2 nm in each propagation direction. The inter-channel timing walk-off is implemented by using a piece of 362-m long standard single mode fiber (SMF). This piece of SMF acts as a dispersive element and induces 20-ps timing walk-off, which is optimal for five 10-Gb/s channels, between every two WDM channels spaced by 3.2 nm in each direction. The ratio of pulsewidth to inter-channel timing walk-off is kept less than 2/3,

which is found to provide sufficient mitigation of the nonlinear inter-channel crosstalks. Thus the pulsewidth of the signals after the synchronous modulation is controlled to be around 13 ps. This can be obtained by cascading additional intensity modulators if necessary in real implementation. It is also noted that the increase of signals' pulsewidth induced by the 362-m SMF is small (less than 0.13 ps). A following EDFA is used for amplification and its gain is optimized to give the best regeneration performance. The amplifier gain was set to be 29 dB in the simulation. The signals are then wavelength-interleaved into two groups by an interleaver, with a channel spacing of 3.2 nm, and launched into the HNLF from the two sides for spectral broadening. The nonlinear coefficient, the zero dispersion wavelength and the dispersion slope of the HNLF are 10.5 $W^{-1} \cdot km^{-1}$, 1550 nm and 0.019 $ps/nm^2/km$, respectively. Both the dispersion and the dispersion slope are sufficiently small so the WDM signals will not experience further significant pulse broadening and walk-off in the HNLF. Finally, both groups of the signals are simultaneously filtered with 0.64-nm offset via using two periodic filters with 0.4-nm bandwidth and 3.2-nm free spectral range. Here the filter offset is optimized for the worst channel. Then the filtered signals are combined for the regenerator output. It is noted that even number of regenerators should be used for the wavelength-preserving inline regeneration.

The regenerative performance of the proposed regenerator operating ten 10-Gb/s WDM channels is investigated. One of the WDM signals degraded by timing jitter (peak-to-peak jitter of 8 ps) and amplitude fluctuations on both the mark and space levels before regeneration is shown in Fig 4.2 (a). With the addition of the synchronous modulation, timing jitter on the original signal is observed to be reduced after regeneration in accompany with the noise suppression on both the mark and space levels when proper inter-channel walk-off is introduced, as shown in Fig 4.2 (b)

and (c) for the best and worst channel respectively. Fig 4.2 (d) gives the totally closed eye of the signal due to the severe nonlinear impairments, in the case that all the WDM pulses coincide in time without proper timing walk-off.

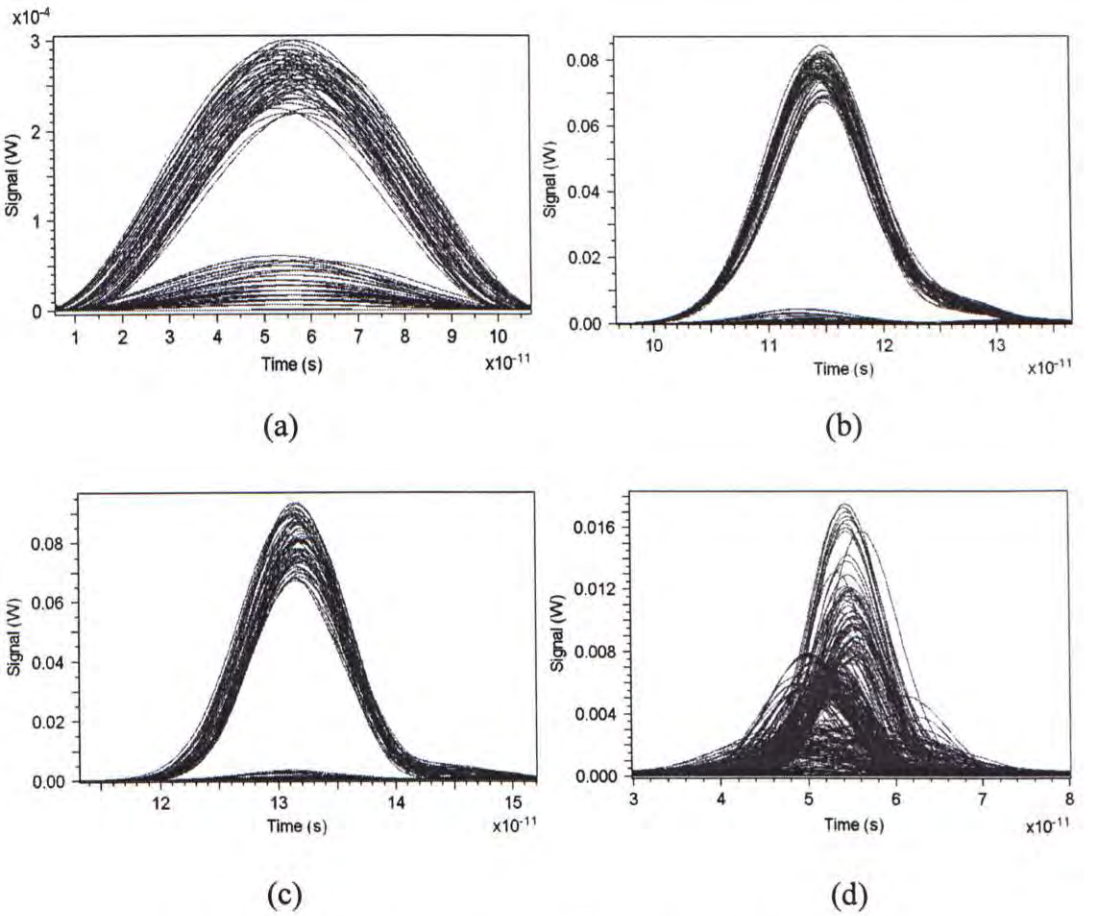

Fig 4.2 (a) Degraded signal of one 10-Gb/s WDM channel before regeneration. (b) and (c) Best and worst channel after 10x10-Gb/s regeneration with proper inter-channel walk-off. (d) Signal after regeneration in the case that all the WDM pulses coincide in time without proper inter-channel walk-off.

The results of the BER measurement are given in Fig. 4.3. We can observe that the regenerative performance of the five-channel operation (unidirectional only) and the ten-channel operation (bidirectional) are close which means the noise caused by Rayleigh backscattering is limited and the use of the bidirectional fiber configuration

induces almost no performance degradation. In addition, the regenerator itself is confirmed to cause little additional penalty to the un-degraded input signals with proper inter-channel timing walk-off. We also see no significant variation of the regenerative performance among different channels and the receiver sensitivity improvement at BER of 10^{-9} is obtained to be 2 to 2.5 dB for the ten-channel operation.

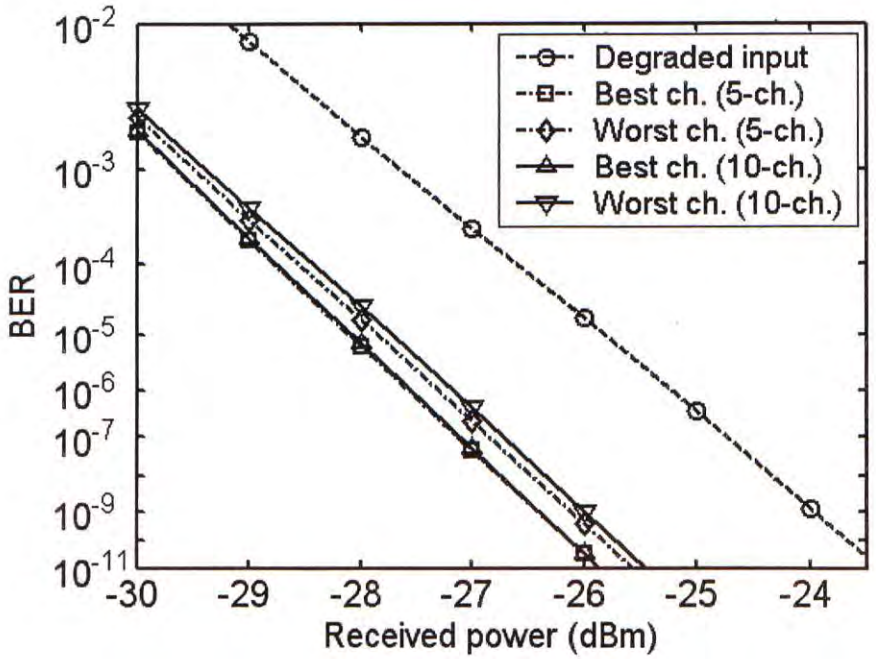

Fig. 4.3 BER measurement of the proposed multi-channel 3R regenerator for 10x10-Gb/s operation by numerical simulations.

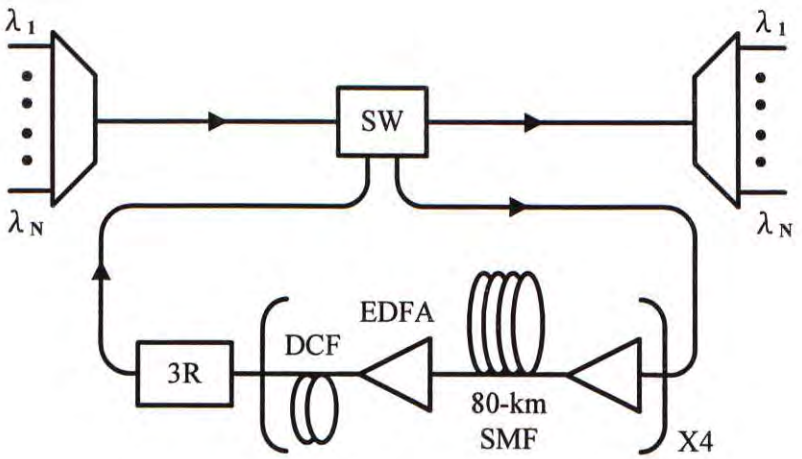

Fig. 4.4 Fiber transmission loop model used in numerical simulations. SW: optical

switch. SMF: single mode fiber; DCF: dispersion compensating fiber.

In order to further investigate the effectiveness of the concatenation of our multi-wavelength 3R regenerator for the need of inline multi-stage regeneration, the fiber transmission loop model shown in Fig. 4.4 is employed in the numerical simulations. The fiber loop consists of four spans of 80-km SMF followed by DCF with full dispersion compensation and our proposed optical 3R regenerator. The total average power launched into the SMF is 2.5 dBm for ten 10-Gb/s WDM channels and the signals' pulsewidth is kept unchanged after each regenerator throughout the whole transmission link. It is worth noting that the requirement of the bit-synchronicity of the WDM channels for the regeneration can be relaxed if we use the RZ-OOK signals with larger duty cycle as the synchronous modulation is employed inside the regenerator. And since the power of different channels may vary after certain transmission distance due to the different attenuation, channel equalization is required to avoid significant performance variation among different channels. Fig. 4.5 shows the BER evolution of the middle channel (at 1542.6 nm) with the increased number of regenerators in the transmission.

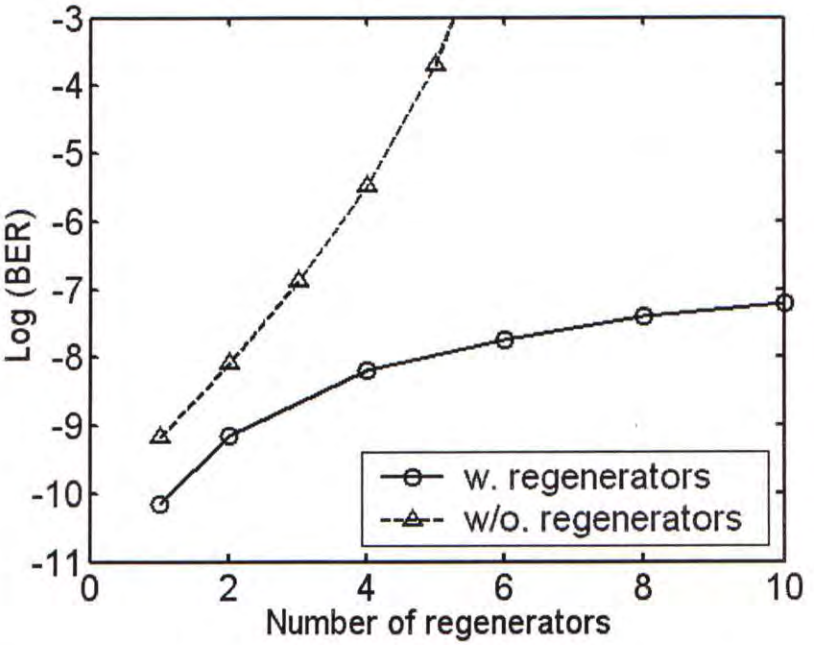

Fig. 4.5 BER evolution of one WDM channel versus the number of the inline regenerators for 10x10-Gb/s regeneration by numerical simulations

We can observe that the BER degrades rapidly without the regenerator due to the accumulated ASE noise, timing jitter and nonlinear impairments. However the use of the regenerators gives a significant increase in the transmission distance with certain acceptable signal quality. The scheme is capable to be further upgraded to support 20 channels if polarization multiplexing is applied.

4.2.2. 4x40-Gb/s scenario

In addition to the capacity upgrade by increasing the channel number, the bit rate on the WDM channels is also possible to be upgraded to a higher speed. In this section, we investigate the performance of the proposed regeneration scheme for operating four 40-Gb/s WDM channels from 1538.4 nm to 1548 nm spaced by 400 GHz.

In the 4x40-Gb/s scenario, only 2 channels are needed to be operated in each propagation direction of the nonlinear fiber inside the regenerator. As a result, the regenerator does not require a big change in the architecture, except that the 362-m SMF, which is used as a dispersive element to introduce 20-ps inter-channel timing walk-off in the 10x10-Gb/s scenario, is now replaced with a piece of 151-m SMF to introduce 12.5-ps inter-channel walk-off for the 40-Gb/s signals in this scenario. It is noted that the pulsewidth of the signals after the synchronous modulation is controlled around 8.2 ps in order to maintain the sufficient mitigation of nonlinear inter-channel crosstalks. In the simulations, both the gain of the EDFA's and the offset of the filter are optimized for the regeneration performance. Fig 4.6 (a) and (b) give the corresponding eye diagrams of the degraded signal before regeneration and after regeneration without proper inter-channel timing walk-off, while (c) and (d) show the best and the worst channels after regeneration with proper inter-channel walk-off respectively in the 4x40-Gb/s operation.

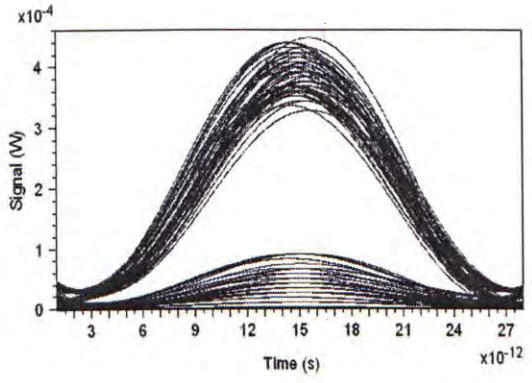

(a)

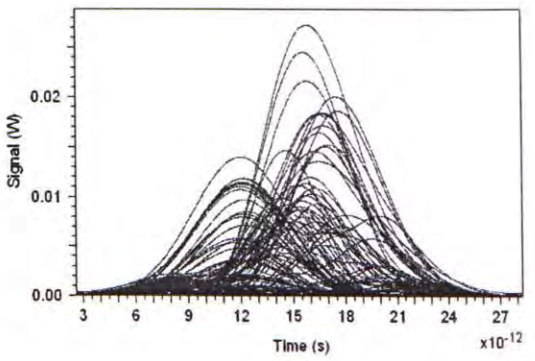

(b)

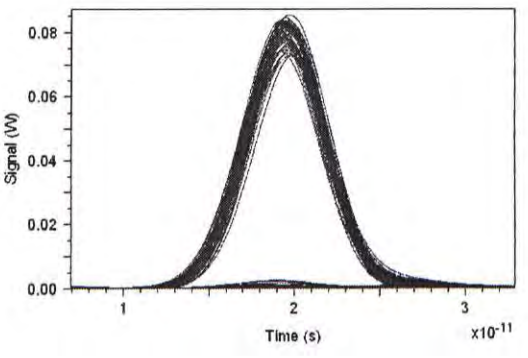

(c)

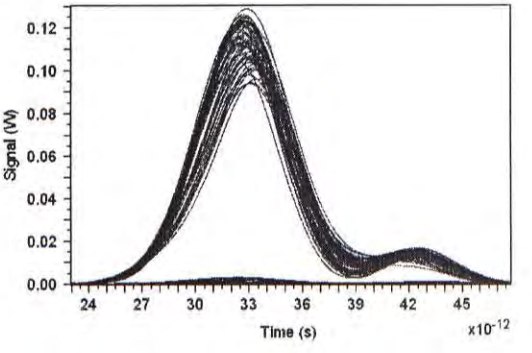

(d)

Fig 4.6 (a) Degraded signal of one 40-Gb/s WDM channel before regeneration. (b) Signal after regeneration without proper inter-channel walk-off. (c) and (d) Best and worst channel after 4x40-Gb/s regeneration with proper inter-channel walk-off.

As can been seen in Fig 4.6 (d), some residual power is observed on the trailing edge of the regenerated signal due to the spectral overlapping (linear crosstalk) of the adjacent WDM channels caused by SPM in the regeneration. However, this residual power actually will not induce eye closesure or significantly affect the quality of the regenerated signals because signals on different wavelengths are already interleaved in time domain by the introduced inter-channel walk-off. Fig 4.7 gives the results of BER measurements for the 4x40-Gb/s operation.

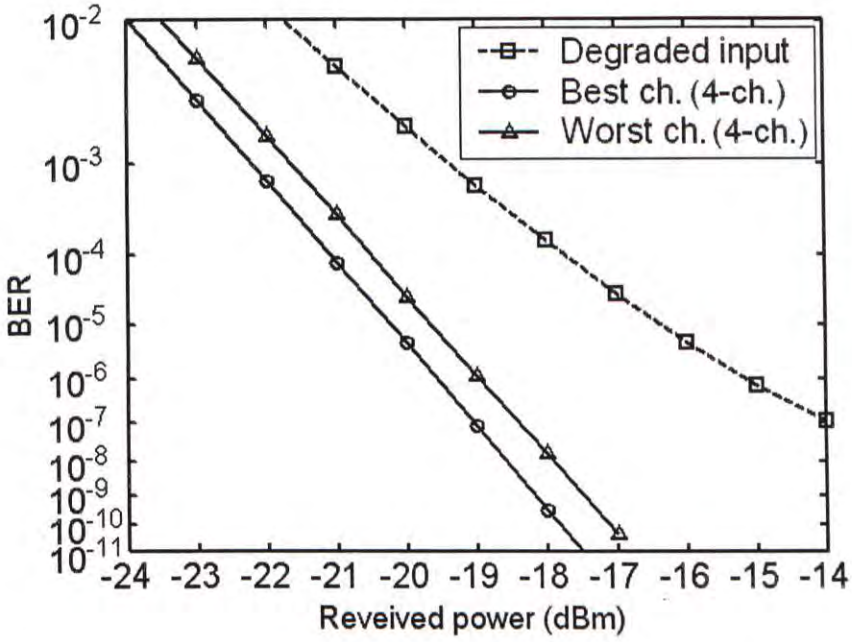

Fig. 4.7 BER measurement of the proposed multi-channel 3R regenerator for 4x40-Gb/s operation by numerical simulations.

Again, we observe neither significant variation of the regenerative performance on different wavelength channels nor Rayleigh backscattering induced power penalty due to the use of bidirectional fiber configuration inside the regenerator. Error-free operations have been achieved for all the channels after the regeneration although the original degraded 40-Gb/s WDM signals are not error-free before regeneration and have an error floor above the BER of 10^{-9}. We have also investigated the cascadability of the regenerator in this 4x40-Gb/s scenario in our simulations using the fiber transmission loop model given in Fig. 4.4. Fig. 4.8 shows the BER evolutions of one WDM channel with the increased number of regenerators in transmission for the 4x10-Gb/s, 10x10-Gb/s and 4x40-Gb/s operation scenarios. We can observe that the BER degrades rapidly without the regenerator due to the accumulated ASE noise, timing jitter and nonlinear impairments for all cases. However the use of the regenerators gives a significant increase in the transmission distance with certain

acceptable signal quality.

In summary, we have demonstrated in numerical simulations that our proposed regeneration scheme is also capable of supporting the capacity upgrade on the data rate of the WDM channels.

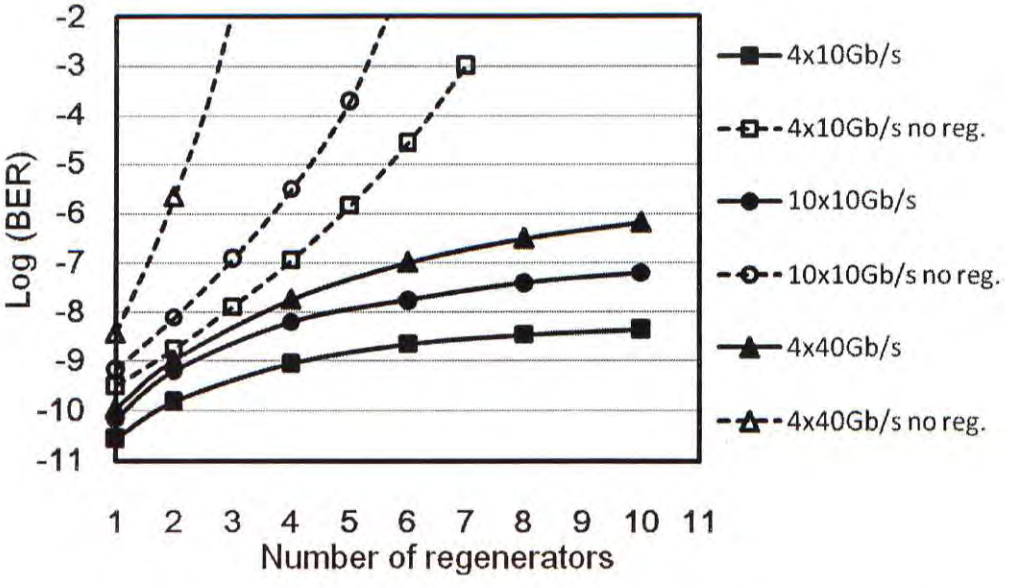

Fig. 4.8 BER evolutions of one WDM channel versus the number of the inline regenerators for different scenarios by numerical simulations.

4.3. Discussions

We have demonstrated in our numerical simulations that our proposed regeneration scheme can work in both the 10x10-Gb/s and the 4x40-Gb/s scenarios. Table 4.1 shows the performance comparison of the regenerator working in these two scenarios. Actually, the regenerator is possible to be further upgraded to support even larger capacity, either by time-interleaving more channels within one signal bit period, or by increasing the bit rate of the WDM channels, thanks to the ultrafast fiber nonlinearities.

However, both these two kinds of capacity upgrade need further narrower signal pulses and the price to pay is a larger channel spacing thus required to prevent the harmful spectral overlapping of adjacent channels caused by SPM in the regeneration. In addition, signals with large frequency spacing are not desirable in the real implementation due to the limited gain bandwidth of EDFAs. It is worth mentioned that the total supported capacity in regeneration can be doubled if polarization multiplexing is employed. As can been seen in Table 4.1, regeneration for the 4x40-Gb/s scenario with a larger total supported capacity and better spectral efficiency seems to be more promising in the next generation high bit-rate WDM systems.

	10x10-Gb/s scenario	4x40-Gb/s scenario
Supported channel no.	10	4
Bit rate of individual channel	10 Gb/s	40 Gb/s
Required channel spacing	200 GHz	400 GHz
Spectral efficiency	0.05 bit/s/Hz	0.1 bit/s/Hz
Total supported capacity	100 Gb/s	160 Gb/s
Sensitivity improvement	2 to 2.5 dB at BER of 10^{-9}	Error-free operation achieved after regeneration for the degraded signals with an error floor at BER of 10^{-9}

Table 4.1 Performance comparison of our proposed regenerator working in the 10x10-Gb/s and the 4x40-Gb/s scenarios

4.4. Summary

In this chapter, we have investigated the scalability of our proposed regeneration scheme and its effectiveness in concatenation for both the 10x10-Gb/s and the 4x40-Gb/s scenarios in numerical simulations. BER measurements show receiver sensitivity improvements of signals in these two scenarios with the use of the regenerator and thus confirms that the proposed regeneration scheme can support both the two kinds of capacity upgrade scenarios. In addition, BER evolution of the signal in transmission with the increased number of regenerators shows that a significant increase in transmission distance for the regenerated signals with certain acceptable quality can be achieved in both these two scenarios. Performance comparison of the regenerator is given upon the two scenarios at last showing the 4x40-Gb/s scenario is more promising in the next generation high bit-rate WDM systems.

Chapter 5 Conclusion and future works

5.1. Summary of the thesis

In this thesis, we have introduced the concept and the functionality of optical signal regeneration technique, and its importance in the optical transmission systems. Some previous schemes of all-optical regeneration based on fiber nonlinear effects and other optical effects in semiconductor devices have been reviewed but those schemes are generally only based on single-wavelength application and thus not suitable in the next generation WDM systems.

As a result, we propose a novel all-optical regeneration scheme that can support the multi-wavelength application based on SPM and inter-channel timing walk-off control. In our experimental demonstration, we have successfully shown that optical 2R regeneration is achieved for four 10-Gb/s WDM channels spaced by 300 GHz because of the successful mitigation of nonlinear inter-channel crosstalks because of the proper inter-channel walk-off introduced.

In addition, in order to further evaluate the scalability of the regenerator and its effectiveness in concatenation for in-line multi-stage regeneration, numerical simulations are carried out and the results show that our regeneration scheme is capable to be upgraded to support either ten 10-Gb/s WDM channels spaced by 200 GHz, or four 40-Gb/s WDM channels spaced by 400 GHz. BER evolution of the

WDM signal in transmission confirms the cascadability of the proposed regeneration scheme with a significant increase in transmission distance when regenerators are used. Performance comparisons of the regeneration schemes for these two capacity upgrade scenarios suggests the 4x40-Gb/s one is more promising in the next generation high bit-rate WDM systems.

5.2. Future works

As what we have described, the scalability investigation of our regeneration scheme in numerical simulations shows that the proposed regenerator has a more promising perspective for four 40-Gb/s WDM channels. This has offered us the orientation of our future research efforts, i.e., to give the experimental demonstration of our regeneration scheme for the 4x40-Gb/s scenario.

Although it is fine for us to use optical tunable delay lines for the inter-channel walk-off control in the 4-channel operations, it is neither efficient nor desirable if the number of channels is increased. When a large number of wavelength channels are involved in the regeneration, a piece of SMF is a desirable choice for introducing the same amount of inter-channel walk-off between WDM channels with the same channel spacing, but it requires the bit-synchronicity of the WDM channels at the regenerator input. As result, our another research goal is to develop a simple and robust technique that can provide tunable delay for multiple wavelength channels simultaneously because this technique would be highly desirable for the bit re-synchronization of the WDM channels and offer a great help in the real implementation of our proposed regenerator. Although the multi-wavelength tunable delay technique has been demonstrated using simulated brillouin scattering-based

(SBS-based) slow light effect in optical fibers, only 2.5-Gb/s amplitude-modulated signals were supported in the scheme due to the limited gain bandwidth of the SBS-generated resonances [42]. We need to explore some other potential candidates for implementation of the multi-wavelength tunable delay. For example: 1) on-chip AWG pairs with integrated phase modulators in between; 2) on-chip silicon micro-ring resonators [43]; 3) micro-electro-mechanical systems (MEMS) with optical gratings [44].

With the use of the multi-wavelength tunable delay technique, a single synchronous modulator is allowed for the re-timing process of all the WDM signals, thus enabling the proposed regenerator to achieve full 3R regeneration of the signals. This is critical especially to the 40-Gb/s systems of which performance is sensitive to the timing jitter.

On the other hand, polarization multiplexing is another straight-forward method to increase the total supported capacity of the regenerator by a factor of 2 by utilizing the polarization-maintaining HNLF and couplers with the polarization controls.

List of publications

[1] Kin-Man Chong and Lian-Kuan Chen, "Optical 3R Regeneration for 10 Synchronous Channels Using Self-Phase Modulation in a Bidirectional Fiber Configuration," *Opto-Electronics and Communications Conference 2009 (OECC'09)*, WD3, 2009.

[2] Kin-Man Chong and Lian-Kuan Chen, "4-Wavelength 2R Regeneration Based on Self-Phase Modulation and Inter-Channel Walk-off Control in Bidirectional Fiber Configuration," *Asia Communications and Photonics Conference and Exhibition 2009 (ACP'09)*, 2009.

Bibliography

[1] Govind P. Agrawal, *Fiber-Optic Communication Systems, 3rd edition*, Wiley inter-science, 2002.

[2] R. Ramaswami and K. N. Sivarajan, *Optical Networks – A Practical Perspective, 2nd edition*, Morgan Kaufmann, 2002.

[3] O. Leclerc, B. Lavigne, E. Balmefrezol, P. Brindel, L. Pierre, D. Rouvillain and F. Segineau, "Optical Regeneration at 40 Gb/s and Beyond," *IEEE J. Lightwave Technol.*, vol. 21, no. 11, pp. 2779-2790, 2003.

[4] John M. Senior, *Optical Fiber Communications – Principles and Practice, 2nd edition*, Prentice Hall, 1992.

[5] P. V. Mamyshev, "All-Opitcal Data Regeneration Based on Self-Phase Modulation Effect," *Proceedings of European Conference on Optical Communication 1998 (ECOC'98)*, pp. 475-476, 1998.

[6] E. Ciaramella and S. Trillo, "All-Optical Signal Reshaping via Four-Wave Mixing in Optical Fibers," *IEEE Photon. Technol. Lett.*, vol. 12, no. 7, pp. 849-851, 2000.

[7] E. Cirarmella, F. Curti and S. Trillo, "All-Optical Signal Reshaping by Means of Four-Wave Mixing in Optical Fibers," *IEEE Photon. Technol. Lett.*, vol. 13, no. 2, pp. 142-144, 2001.

[8] A. Bogris and D. Syvridis, "Regenerative Properties of a Pump-Modulated Four-Wave Mixing Scheme in Dispersion-Shifted Fibers," *IEEE J. Lightwave Technol.*, vol. 21, no. 9, pp. 1892-1902, 2003.

[9] N. Chi, L. Xu, K. S. Berg, T. Tokle and P. Jeppesen, "All-Optical Wavelength Conversion and Multichannel 2R Regeneration Based on Highly Nonlinear

Dispersion-Imbalanced Loop Mirror," *IEEE Photon. Technol. Lett.*, vol. 14, no. 11, pp. 1581-1583, 2002.

[10] M. Matsumoto, "Simultaneous reshaping of OOK and DPSK signals by a fiber-based all-optical regenerator," *Opt. Express*, vol. 14, no 4, pp. 1430-1438, 2006.

[11] Y. O. Kim, J. H. Lee, J. M. Kang and S. K. Han, "2R limiter circuit with gain clamped SOA for XGM wavelength converter," *IEE proceedings of Optoelectronics*, vol. 152, no. 1, pp. 11-15, 2005.

[12] M. Spyropoulou, S. Sygletos, I. Tomkos, "Simulation of Multiwavelength Regeneration Based on QD Semiconductor Optical Amplifiers," *IEEE Photon. Technol. Lett.*, vol. 19, no. 20, pp. 1577-1579, 2007.

[13] M. Spyropoulou, S. Sygletos, I. Tomkos, "Study of a Multi-wavelength Regenerative subsystem based on Quantum Dot Semiconductor Optical Amplifiers at 40Gbps," *Proceedings of Optical Fiber Communication Conference 2007 (OFC'07)*, pp. 1-3, 2007.

[14] J. F. Pina, H. Silva, P. N. Monteiro, J. Wang, W. Freude, J. Leuthold, "Cross-Gain Modulation-based 2R Regenerator Using Quantum-Dot Semiconductor Optical Amplifiers at 160 Gbit/s," *Proceedings of International Conference on Transparent Opitcal Networks 2007 (ICTON'07)*, pp. 106-109, 2007.

[15] Sune Højfeldt, Svend Bischoff, and Jesper Mørk, "All-Optical Wavelength Conversion and Signal Regeneration Using an Electroabsorption Modulator," *IEEE J. Lightwave Technol.*, vol. 18, no. 8, pp. 1121-1127, 2000.

[16] L. Huo, Yanfu Yang, Yinbo Nan, Caiyun Lou, and Yizhi Gao, "A Study on the Wavelength Conversion and All-Optical 3R Regeneration Using Cross-Absorption Modulation in a Bulk Electroabsorption Modulator," *IEEE J. Lightwave Technol.*, vol. 24, no. 8, pp. 3035-3044, 2006.

[17] K. Nishimura, M. Tsurusawa, M. Usami, "Noval all-optical 3R regenerator using cross-absorption modulation in RF-driven electroabsorption waveguide", *Proceeding of European Conference on Optical Communication 2001 (ECOC' 01)*, pp. 286-287, 2001.

[18] Ch. Kouloumentas, P. Vorreau, L. Provost, P. Petropoulos, W. Freude, J. Leuthold and I. Tomkos, "All-Fiberized Dispersion-Managed Multichannel Regeneration at 43 Gb/s," *IEEE Phonton. Technol. Lett.*, vol. 20, no. 22, pp. 1854-1856, 2008.

[19] Govind. P. Agrawal, *Nonlinear fiber optics, 3rd edition*, San Diego: Academic Press, 2001.

[20] A. Bogoni, P. Ghelfi, M. Scaffardi, and L. Poti, "All-optical regeneration and demultiplexing for 160-Gb/s transmission systems using a NOLM-based three-stage scheme," *IEEE J. selected topics in Quantum Electron.*, vol. 10, no. 1, pp. 192–196 (2004).

[21] M. Matsumoto, Y. Shimada, H. Sakaguchi, "Two-Stage SPM-Based All-Optical 2R Regeneration by Bidirectional Use of a Highly Nonlinear Fiber," *IEEE J. Quantum Electron.*, vol. 45, no. 1, pp. 51-58, 2009.

[22] T. N. Nguyen, M. Gay, L. Bramerie, T. Chartier, J. C. Simon, "Noise reduction in 2R-regeneration technique utilizing self-phase modulation and filtering," *Opt. Express*, vol. 14, no. 5, pp. 1737-1747, 2006.

[23] P. Petropoulos, *et al.*, "Simultaneous 2R Regeneration of WDM Signals in a Single Optical Fibre," *Proceedings of IEEE/LEOS Winter Topicals Meeting Series*, pp. 252-253, 2009.

[24] D. V. Kuksenkov, S. Li, M. Sauer, D. A. Nolan, "Nonlinear fibre devices operating on multiple WDM channels," *Proceeding of European Conference on Optical Communication 2005 (ECOC'05)*, pp. 51-54, 2005.

[25] M. Vasilyev, T. I. Lakoba, "All-optical multichannel 2R regeneration in a

fiber-based device," *Opt. Lett.*, vol. 30, no. 12, pp. 1458-1460, 2005.

[26] L. Provost, F. Parmigiani, P. Petropoulos, D. J. Richardson, K. Mukasa, M. Takahashi, J. Hiroishi, M. Tadakuma, "Investigation of Four-Wavelength Regenerator Using Polarization- and Direction-Multiplexing," *IEEE Photon. Technol. Lett.*, vol. 20, no. 20, pp. 1676-1678, 2008.

[27] Kin-Man Chong and Lian-Kuan Chen, "Optical 3R Regeneration for 10 Synchronous Channels Using Self-Phase Modulation in a Bidirectional Fiber Configuration," *Opto-Electronics and Communications Conference 2009 (OECC'09)*, WD3, 2009.

[28] Ning Deng, Kit Chan, Chun-Kit Chan, Lian-Kuan Chen, "An all-optical XOR logic gate for high-speed RZ-DPSK signals by FWM in semiconductor optical amplifier," *IEEE J. selected topics in Quantum Electron.*, vol. 12, no. 4, pp. 702-707, 2006.

[29] Zhihong Li, Guifang Li, "Ultrahigh-speed reconfigurable logic gates based on four-wave mixing in a semiconductor optical amplifier," *IEEE Photon. Technol. Lett.*, vol. 18, no. 12, pp. 1341-1343, 2006.

[30] A. Bogoni, L. Poti, R. Proietti, G. Meloni, F. Ponzini, P. Ghelfi, "Regenerative and reconfigurable all-optical logic gates for ultra-fast applications," *Electron. Lett.*, vol. 41, no. 7, pp. 435-436, 2005

[31] L. Rau, Wei Wang, B. E. Olsson, Yijen Chiu, Hsu-Feng Chou, D. J. Blumenthal, J. E. Bowers, "Simultaneous all-optical demultiplexing of a 40-Gb/s signal to 4×10 Gb/s WDM channel's using an ultrafast fiber wavelength converter," *IEEE Photon. Technol. Lett.*, vol. 14, no. 12, pp. 1725-1727, 2002.

[32] T. Sakamoto, K. Seo, K. Taira, N. S. Moon, K. Kikuchi, "Polarization-insensitive all-optical time-division demultiplexing using a fiber four-wave mixer with a peak-holding optical phase-locked loop," *IEEE Photon. Technol. Lett.*, vol. 16,

no. 2, pp. 563-565, 2004.

[33] Jifang Qiu, Guangtao Zhou, Jian Wu, Jintong Lin, "8x10 Gb/s OTDM Signal Demultiplexing by Using Self-Cascaded Electro-Absorption Modulator (EAM) After Transmitting Over 300 km," *IEEE Photon. Technol. Lett.*, vol. 18, no. 23, pp. 2541-2543, 2006.

[34] M. Y. Jeon, D. S. Lim, H. K. Lee, J. T. Ahn, D. I. Chang, K. H. Kim, S. B. Kang, "All-optical wavelength conversion for 20-Gb/s RZ format data," *IEEE Photon. Technol. Lett.*, vol. 12, no. 11, pp. 1528-1530, 2000.

[35] A. Uchida, M. Takeoda, T. Nakata, F. Kannari, "Wide-range all-optical wavelength conversion using dual-wavelength-pumped fiber Raman converter," *IEEE J. Lightwave Technol.*, vol. 16, no. 1, pp. 92-99, 1998.

[36] Jianjun Yu, Xueyan Zheng, C. Peucheret, A. T. Clausen, H. N. Poulsen, P. Jeppesen, "All-optical wavelength conversion of short pulses and NRZ signals based on a nonlinear optical loop mirror," *IEEE J. Lightwave Technol.*, vol. 18, no. 7, pp. 1007-1017, 2000.

[37] N. Edagawa, M. Suzuki, and S. Yamamoto, "Novel wavelength converter using an electroabsorption modulator," *IEICE Trans. Electron.*, vol. E81-C, no. 8, pp. 1251–1257, 1998.

[38] T. Otani, T. Miyazaki, and S. Yamamoto, "40-Gb/s optical 3R regenerator using electroabsorption modulators for optical networks," *IEEE J. Lightwave Technol.*, vol. 20, no. 2, pp. 195–200, Feb. 2002.

[39] H. Tanaka, M. Hayashi, T. Otani, K. Ohara, and M. Suzuki, "60 Gb/s WDM-OTDM transmultiplexing using an electro-absorption modulator," *Proceedings of OFC'01*, pp. ME4-1–ME4-3, 2001.

[40] M. Nakazawa, E. Yamada, H. Kubota, K. Suzuki, "10 Gbit/s soliton data transmission over one million kilometres," *Electorn. Lett.*, vol. 27, no. 14, pp.

1270-1272, 1991.

[41] Q. Yu and A. Shanbhag, "Electronic Data Processing for Error and Dispersion Compensation," *IEEE J. Lightwave Technol.*, vol. 27, no. 12, pp. 4514-4525, 2006.

[42] B. Zhang, L.-S. Yan, J. Y. Yang, I.Fazal and A. E. Willner, "A Single Slow-Light Element for Independent Delay Control and Synchronization on Multiple Gb/s Data Channels," *IEEE Photon. Technol. Lett.*, vol. 19, no. 14, pp. 1081-1083, 2007.

[43] Q. Li, F. Liu, Z. Zhang, M. Qiu and Yikai Su, "System Performances of On-Chip Silicon Microring Delay Line for RZ, CSRZ, RZ-DB and RZ-AMI Signals," *IEEE J. Lightwave Technol.*, vol. 26, no. 23, pp. 3744-3751, 2008.

[44] T. Sano, et al., "Novel Multichannel Tunable Chromatic Dispersion Compensator Based on MEMS and Diffraction Grating," *IEEE Photon. Technol. Lett.*, vol. 15, no. 8, pp. 1109-1110, 2003.